



Isotherm Modeling Of the Removal of Lead and Cadmium Ions from Pharmaceutical Wastewater Using Oil Palm Empty Fruit Bunch

Engr. Dr. C. Odenigbo¹ & Agu, Emeka Micheal²

¹Civil Engineering Department, Enugu State University of Science and Technology ESUT, Enugu.

²Public Complaints Commission

ABSTRACT: This review prioritized isotherm modelling of the lead and cadmium purging from pharmaceutical wastewater using activated oil palm empty fruit bunch. The heavy metals in pharmaceutical wastewater sample were revealed by the Atomic Absorption Spectrometry analysis, which proved that lead and cadmium metals are the most dangerous metals in the sample under analysis because they exceed the acceptable limits given by World Health Organization. The nutritional value of the raw and activated oil palm bunch, revealed through proximate analysis, indicated an increase in adsorbent properties after chemical activation. The surface morphological perusal of the raw and activated samples revealed considerable increment in the number of the vacant pores for effective adsorption post acid treatment while the Fourier Transform Infrared Spectrometer analysis also indicated a surge in void spaces after activation as a result of the disappearance of certain functional groups. Kinetic, thermodynamic and isotherm modeling of the purging of lead and cadmium from pharmaceutical effluents by adsorption were done using standard equations. Langmuir model closely followed by Temkin model were the most fitting models for the adsorption process. Pseudo-second order kinetic model is the most suitable kinetic model while the results from the thermodynamic study, such as change in enthalpy, change in entropy and standard Gibb's free energy indicated the non-spontaneity of the process. Batch adsorption study experiment was used to ascertain the effects of stirring time, temperature and dosage of the activated palm bunch on the lead and cadmium ions removal. These process conditions were optimized with central composite design of response surface methodology with the aid of a design expert (version 13). The response was removal efficiency while the suggested model was quadratic. The predicted removal efficiencies of the adsorbent for lead and cadmium ions are 89.234% and 73.318% respectively at 69.150mins, 345.155°C and 0.266g adsorbent dosage. This was validated by carrying out the metal removal at the suggested conditions to obtain actual adsorbent removal efficiencies of 87.82% and 72.51% for lead and cadmium respectively. Thus, activated oil palm bunch is economically viable and practically proven biomass waste for pharmaceutical wastewater treatment.

Keywords: Industrial effluents, waste-water, contaminants, pharmaceutical effluents, Biomass.

Received 03 June, 2023; Revised 11 June, 2023; Accepted 13 June, 2023 © The author(s) 2023.

Published with open access at www.questjournals.org

I. INTRODUCTION

The earth-crust has been scientifically proven to be made up of 70% water, however the natural compositions of most of these water bodies are clear indications that they are unsafe for drinking purposes. The scenario has even been worsened by industrial and household activities especially since the turn of the 20th century. The contamination of our water bodies is as a result of the deposition of large quantity of industrial effluents/wastewaters (Che et al., 2018). Water pollution is majorly due to the release of discharge from domestic and industrial activities. These discharge contaminants could be chemicals, heavy metals, pigments, dyes, pathogenic organisms and many carcinogenic substances, which have serious health hazards effects (Qin et al., 2015; Adebisi et al., 2007; Bakare et al., 2003). This is a global concern because the contamination of oceans and rivers by the wastewater discharge (Shirafkan et al., 2016) has limited the availability of portable drinking water and clean water for the survival of aquatic lives (Cerro-Lopez & Méndez-Rojas, 2017; Lee et al., 2017).

Since water is an important raw material in almost all industrial operations, therefore every industry generates wastewater. Pharmaceutical industries generate large amount of wastewaters because they use water to carry out many activities and operations. Pharmaceutical effluents are those effluents resulting from the actual pharmaceutical operations such as drug manufacturing (Chimezie et al., 2011). There are large varieties of products in pharmaceutical wastewaters because the production of pharmaceutical compounds is done in batches. These varying product particles are obtained in different operations because of the fact that large quantities of water, which are used for solid cake washing, extraction purposes, equipment washing and the actual production process. Pharmaceutical particles in urban and rural wastewaters are mainly due to the production process of pharmaceutical companies and common use of pharmaceutical compounds by people. Pharmaceutical industries are among the major industries that discharge large quantity of wastewater into the environment. Other industries are plastic, petroleum, rubber, fertilizer production industries, steel, coal and mining industries (Loredo-Cancino et al., 2016). Most pharmaceutical compounds are artificially made and classified very dangerous due to their high biological oxygen demand (BOD), chemical oxygen demand (COD), dissolved and suspended solids, chlorides, sulphides, phenols, oils and heavy metals such as cadmium, zinc, lead, iron, mercury, aluminium, arsenic, manganese, chromium and nickel (Rana et al., 2017; Gupta SK & Hung YT, 2006; Fawzy et al., 2018; Sitre et al., 2009). These heavy metal even low concentrations have significant pollutant effects of our ecosystem (Alslaibi et al., 2015). Their non-biodegradability and ease of accumulation into plant and animal tissues makes them worrisome water pollutants. This study will primarily focus on the purging of lead and cadmium impurities from the pharmaceutical wastewaters. Cadmium is one of the heavy metals, which is highly toxic to human, plants and animals, and these unhealthy effects cannot be ignored because the metal is not degradable. The tendency of cadmium to easily displace important metals such as zinc and calcium when it combines with sulfur makes cadmium a highly toxic effect (Memon et al., 2007).

Many wastewater treatment technologies have been proposed in literature but recent research trends favour adsorption technology using waste biomass as adsorbents. This review will explore the efficacy of oil palm empty fruit bunch in the removal of lead and cadmium ion impurities from the pharmaceutical wastewater. The interest in oil palm empty fruit bunch in Nigeria is huge because of its abundance. The waste is generated in sizeable quantity in Nigeria because Nigeria is among the top four producing palm oil countries. Moreover, aside being used as fuel to set up fire (which is an unhealthy act leading to atmospheric pollution), it has no other application in Nigeria. Recently, oil palm empty fruit bunch has been considered an effective adsorbent for water treatment because it is rich in carbon and has high cellulose, hemicellulose and lignin contents (Thoe et al., 2019). The adsorption capacity of oil palm empty fruit bunch like many other carbon based materials can be improved through carbonization and chemical activation processes (Mohamad et al., 2013; Zhang et al., 2017).

II. HISTORICAL BACKGROUND

Sizeable amount of wastewaters is due to industrial operations because most water bodies are easily contaminated by the unruly discharge of industrial wastes (Che et al., 2018), in the form of by-products, chemicals, metal impurities and effluents (Qin et al., 2015; Rana et al., 2017). The pollution of large water bodies like oceans and rivers by these industrial discharges have detrimental health effects because we need pure water for drinking and other crucial life activities (Cerro-Lopez & Méndez-Rojas, 2017; Lee et al., 2017). Nigeria is among the top developing countries ravaged by the discharge of industrial effluents (Ohioma, et al., 2009), especially from pharmaceutical industries due to poor industrial waste management. Most pharmaceutical compounds are known to contain heavy metals, such as cadmium, zinc, lead, iron, mercury, aluminum, arsenic, manganese, chromium and nickel (Rana et al., 2017; Fawzy et al., 2018). In the past, many conventional wastewater treatment technologies to remove heavy metal impurities have been used, even though, some of the technologies proved very efficient, the whole process is not feasible in Nigeria due to poor economy and technical know-how. Some advance treatment technologies such as electrochemical method, membrane separation process, etc, are not viable here due to cost of installation, operation and maintenance cost. Thus, application of adsorption treatment method using cheap and natural biomass as adsorbents has gained sufficient ground recently. This is even more interesting as these biomasses are generated in very large quantities and in most cases are discarded as wastes, which pose serious environment ill-health problem. Thus, utilizing these agro-based biomass wastes solves the immediate problem of poor waste management and disposal; and at the same time, offers indigenous pharmaceutical companies affordable means of maintaining treating their wastewaters and effluents.

BIOMASS

Biomass is a collective term used for all materials that are biogenic in origin, i.e. derived from the product of photosynthesis. Biomass can be of various types; it can have plant/animal origin (Quaak and Knoef, 1999). The earliest and commonest source of energy known to human is biomass. Biomass could be described as the total mass of living organisms, bacteria and plankton, advanced vegetal, mammals and human beings. All

the matter produced by biological organisms can be considered biomass, even for energetic applications. The term biomass also includes a wide range of materials, from plastic bags to agricultural wastes. Biomass for energy use can be classified into industrial waste, landfill gas, agricultural crops, wooden biomass and alcohol fuels (Quaak and Knoef, 1999).

Oil Palm Empty Fruit Bunch: In a typical palm oil mill, empty fruit bunches are abundantly available as a fibrous material of purely biological origin. It is one of the lignocellulosic materials, which has great relevance since a large quantity of the biomass is generated by oil palm industries (Chinomso & Isaac, 2012). The empty fruit bunches are considered as unwanted waste. In the oil extraction process, the fruits or nuts are first stripped from fruit bunches, leaving behind the empty fruit bunch as waste. EFB contains neither chemical nor mineral additives, and depending on proper handling operations at the mill, it is free from foreign elements such as gravel, nails, wood residues (Nordin et al., 2013). As a major waste in Nigeria oil palm producing companies, they don't have much other applications aside used as fuels to set up fire in traditional means of cooking in rural areas. This has been banned in most developed countries as the soot generated in the process is not healthy since it is a huge source of air pollution. Thus, making landfilling the only disposal option. This act is not 100% safe on long run and was later deemed nutrient loss because this waste can be recycled to give nutrients to the soil (Abu bakar et al., 2011). This act of converting this waste into value added products is not viable due to high cost (Thoe et al., 2019). Recently, oil palm empty fruit bunch has been considered an effective adsorbent for water treatment because it is rich in carbon and has high cellulose, hemicellulose and lignin contents (Thoe et al., 2019).

Composition of oil palm empty fruit bunch

The range of the properties of oil palm empty fruit bunch, according to some literatures, is shown in Table 2.1:

Table 2.1: Characteristics of raw oil palm empty fruit bunch

Table 2.1 showed wide ranges in properties compositions. Thus the properties of the oil palm empty fruit bunch are affected by topography, sample origin, nature and fertility of the soil, weather conditions and soil nutrients (Janice et al., 2019).

Biomass and Metallic Ions Interactions

A lot of concerns have been raised globally over the rising cases of heavy metallic ions from different industrial operations (Rangsayatorn et al., 2004). These metals do not degrade and they are very difficult to destroy. So the

Parameters	Range	Source
C	40.93 - 68.2	Idris et al., (2010); Yang et al., (2004)
H	2.88 - 7.33	Wahi et al., (2009); Mohammed et al., (2012)
S	0.04 – 0.92	Parshetti et al., (2013)
N	<0.1 – 2.18	Shariff et al, (2014); Abdullah & Sulaiman, (2013)
O	2.64 – 51.78	Idris et al., (2010)
Lignin	10 – 34.37	Abdullah & Sulaiman, (2013)
Hemicellulose	19.5 – 38.8	Coral Medina et al., (2015);
Cellulose	22.2 – 65	Mohammed et al, (2012); Mahjoub et al., (2012)
Ph	7.10 - 7.80	Kavitha et al., (2013);

only option is to remove them.

PHARMACEUTICAL INDUSTRY AND PHARMACEUTICAL WASTEWATER OVERVIEW

Pharmaceutical products, once used or expired, are considered a special type of waste in the environment that have been catalogued as chemicals of emerging concern to the public because of their potential to pollute water (WHO, 2006; Sarici-Özdemir and Önal 2010; Bagheri et al., 2014). The global pharmaceutical consumption is estimated as ~1,000,000 tons/year with 15 g/year as per capita use (Wei et al., 2020). Several pharmaceutical molecules cannot be totally absorbed and metabolized, thus, they are excreted and released to the environment. Therefore, a significant amount of pharmaceuticals are released into the surroundings during its production, delivery, use, application, and excretion (WHO 2006; Yu et al., 2017). Pharmaceutical molecules could be found in concentrations ranging from ng/L to µg/L in ground waters, wastewaters, and surface waters (Yu et al., 2017). Wastewaters could contain significant amounts of more than 55 pharmaceuticals over the 150 daily used compounds (Sui et al., 2015; Huerta-Fontela et al., 2011; Hounfodji et al., 2021). The bioaccumulation of these compounds represents a serious eco-toxicological risk and implies adverse effects like organism drug resistance, metabolism disruptions, and bacteria strain proliferation (Shao et al., 2012; Hounfodji et al., 2021; Liu et al., 2019). The concentration of pharmaceutical compounds can be effectively reduced in water via adsorption (Wei et al., 2020).

Pharmaceutical industry encompasses production, processing, purification and packaging of materials whether chemical and biological or whether in solid or liquid form for human and animals' medication. Majority of the active pharmaceutical ingredients are manufactured by chemical synthesis involving organic, inorganic

and biological reactions. The processes of drug formulation and manufacturing give rise to pharmaceutical wastewater.

Classification of Pharmaceutical Industries

Pharmaceutical industries could be classified into five categories based on the different manufacturing processes: (1) Fermentation plants (2) Synthesized organic chemical plants (3) Fermentation/synthesized organic chemical plant (4) Natural/biological product extraction plants (antibiotics/vitamins/enzymes, etc.) and (5) Drug mixing, formulation and preparation plants (tablets, capsules and solutions, etc.).

PROCESSES INVOLVED IN PHARMACEUTICAL MANUFACTURING

Chemical synthesis process: Here the batch operations for producing drugs with specific action use organic and inorganic chemicals. A series of chemical reactions are done in multipurpose reactors. This process consists of many steps with a lot of intermediates and by-products. Different separation processes, such as leaching, filtration, crystallization and liquid-liquid extraction, are used in the isolation of the products, after which the separated product is dried, milled and sent to the formulation unit for further processing. Large amount of wastewaters is generated in chemical synthesis process because of many processes and operations occurring in the reactor. Moreover, there are many stages and each stage involves the production of liquor containing unreacted materials, unwanted products, by-products and residual solvent in the organic solvent base. Wastewater is produced at the purification steps and it is made up of solvents, finished products, by-products and spills.

Fermentation process: This is a biochemical process that produces a chemical substance using yeast, lactic acid bacillus and micro-organism. It can take place in batches. There are three steps in batch fermentation process. The steps are seed inoculum and preparation, fermentation and product recovery.

RECENT TECHNOLOGIES USED IN PHARMACEUTICAL WASTEWATER TREATMENT

There are variations in composition, quality and quantity of wastewaters generated from pharmaceutical industries, depending on the season, time, raw materials, location and processes used during production of many drugs. Hence it is very difficult to specify a particular treatment system for such a diversified pharmaceutical industry. Many alternative treatment processes are available to deal with the wide array of waste produced from this industry, but they are specific to the type of industry and associated wastes. Different methods of heavy metals removal from water bodies and wastewater have been adopted which include membrane filtration, ion exchange/solvent extraction, electrochemical operations, reverse osmosis, coagulation/filtration, evaporation, electrolysis, chemical precipitation etc. (Yang and McGarrhian, 2005; Gupta et al., 2004; Nordberg et al., 2007).

Table 2.2: Advantages and disadvantages of different methods of wastewater treatment

Treatment Method	Merits	Demerits
Ion Exchange	Efficient in metal selection. Easy materials regeneration.	Expensive. Removes fewer metals.
Membrane Technology	Solid waste production. Consumes less materials. 95% efficiency for single metal.	Concentrated sludge is produced. Efficiency decreases with time. Reduced flow-rate. Expensive to start-up and operate.
Chemical Coagulation	Sludge settlement. Dewatering. Easy metal selection.	Very expensive. High chemical consumption..
Electrochemical Means	Not complex. Consumes no chemical. Easily separates pure metals.	Expensive to start-up and operate.
Chemical Precipitation	Affordable. Remove most metals.	Large sludge is produced. Disposal difficulty.
Oxidation	Quick toxic pollutants removal.	Requires high energy. Formation of by-product.
Ozonation	Applied in gaseous phase. Reduction of volume.	Reduced half-life.
Biological Treatment	Active in removing the selected metals.	Commercialized technology still in view.
Photochemical	No sludge is produced. Requires no energy for activation of H ₂ O ₂ .	By-product formation.
Fenton Reagents	High removal efficiency.	Sludge is produced.
Irradiation	Effective for separation in the laboratory.	A lot of dissolved oxygen is required.

ADSORPTION

The mitigation of environmental pollution from wastewater using adsorption technology has gained considerable attention and recognition in industries (Abasi et al., 2011; Sarin et al., 2004).

Two main classification of adsorption technique are physisorption and chemisorption.

Physisorption: This is described as physical adsorption that involves Van der Waals forces which do not require a considerable transformation in the electronic orbital arrangements of the species (Nabais, 2006).

Physisorption produces equal energy potential emanating from the adsorbent and the adsorbate but greater than the condensation energy released by the adsorptive; thus, no activation energy is required. In cases of physisorption, the reactions are favoured at low temperatures; therefore, physisorption process decreases with increase in temperature (Al-Anber, 2007). Also, in physisorption, equilibrium exists between the fluid phase and the adsorbate resulting in multilayer adsorption.

Chemisorption: This is referred to as chemical adsorption where the adsorption process is propagated by chemical bonds forged between the adsorbent and the adsorbate. Energies are dissipated like that of chemical reaction which may be endothermic or exothermic resulting in either small or large energy magnitudes. Its preliminary step requires enormous activation energy (Activated adsorption), which indicates that the pace at which equilibrium is attained may be reduced. Chemisorption process is favoured at high temperatures. Usually, chemisorbed species can be removed from the surface either by extreme temperature conditions or high exhaustion or the application of chemicals on the surface. The adsorption sites on the surface are usually occupied with layers formed by the chemo – adsorbed material (Kong, 2009). When the monomolecular layer covers the surface, the adsorbent is said to be essentially depleted. In addition, movement of molecules from one surface to the other is limited (Kong, 2009). The adsorption process is irreversible.

Commercial Adsorbents

Some adsorbents have been extensively explored for controlling water pollution. They are zeolite, Silica gel, and activated carbon.

SOME IMPORTANT ANALYSIS AND CHARACTERIZATION TOOLS

Scanning electron microscopy (SEM): This is also known as SEM analysis or SEM technique. It can be regarded as an effective method in analysis of organic and inorganic materials on a nanometer to micrometer (μm) scale. SEM works at a high magnification reaches to 300,000x and even 1000000 (in some modern models) in producing images very precisely of wide range of materials. SEM is a tool at which invisible worlds of microspace and nanospace can be seen. Details and complexity that is inaccessible by light microscopy can be revealed by SEM.

Fourier Transform Infrared Spectroscopy: This has wide range of application, such as analysis of small molecules and tissues or cells. It is used for the mapping of cellular components (carbohydrates, lipids, proteins) to identify abnormal cells (Levin and Bhargava 2005; Petibois & De le'ris 2006).

PROCESS MODELING AND OPTIMIZATION

Adsorption Isotherms

Adsorption isotherms provide basic information on the nature of interaction between the inhibitor and the metal through applying some adsorption isotherm models. Holistically, adsorption isotherms showcase two categories of adsorption namely; (i) reversible (comprising of physical adsorption and weak chemical adsorption) and (ii) irreversible (actively chemisorbed) (Al-Anber and Al-Anber, 2008; Al – Anber, 2007).

Occasionally, both physical adsorption and chemical adsorption may occur simultaneously or adversely, a film of molecule may undergo physisorption above an elemental chemisorbed film (Denizli et al., 2000).

a) Langmuir Adsorption Isotherm

Langmuir adsorption isotherm describes the quantitative formation of a monolayer adsorbate on the outer surface of the adsorbent. It is the most suitable for physical and chemical adsorption where there is no interaction between the adsorbate and adsorbent. Thereby, the Langmuir may represent the equilibrium distribution of metal ions between the solid and liquid phases. The model assumes uniform energies of adsorption onto the surface and no transmigration of adsorbate in the plane of the surface. Based upon these assumptions, Langmuir represented the following equation:

$$q_e = \frac{Q_0 K_L C_e}{1 + K_L C_e} \quad (q_e =$$

$$\frac{Q_0 K_L C_e}{1 + K_L C_e}) \quad (2.1)$$

Langmuir adsorption parameters were determined by transforming the Langmuir equation 2.11 into linear form:

$$\frac{1}{q_e} = \frac{1}{Q_0} + \frac{1}{Q_0 K_L C_e} \frac{1}{q_e} = \frac{1}{Q_0} + \frac{1}{Q_0 K_L C_e} \quad (2.2)$$

Where: C_e = the equilibrium concentration of adsorbate (mgL^{-1})

q_e = the amount of metal adsorbed per gram of the adsorbent at equilibrium (mg/g).

Q_o = maximum monolayer coverage capacity (mg/g)

K_L = Langmuir isotherm constant (L/mg).

b) Freundlich Adsorption Isotherm:

This is commonly used to describe the adsorption characteristics for the heterogeneous surface. The empirical equation proposed by Freundlich is given by:

$$Q_e = K_f C_e^{1/n} \quad (2.3)$$

Where K_f = Freundlich isotherm constant (mg/g)

n = adsorption intensity;

C_e = the equilibrium concentration of adsorbate (mg/L)

Q_e = the amount of metal adsorbed per gram of the adsorbent at equilibrium (mg/g). Linearizing equation 2.36, we have:

$$\log Q_e = \log K_f + \frac{1}{n} \log C_e \quad (2.4)$$

The constant K_f is an approximate indicator of adsorption capacity, while $1/n$ is a function of the strength of adsorption in the adsorption process (Voudrias et.al, 2002). However K_f and n are parameters characteristic of the sorbent-sorbate system, which must be determined by data fitting, and where linear regression is generally used to determine the parameters of kinetic and isotherm models (Guadalupe, 2008). However, when $\frac{1}{n} = 1$, the relation becomes a linear adsorption isotherm. There is a favorable sorption process when the values of n lies in between one and ten (Goldberg, 2005).

c) Temkin Isotherm:

This model suggests that the heat of adsorption (function of temperature) of all molecules in the layer would decrease linearly rather than logarithmic with the surface coverage.

Adsorption Kinetics

Adsorption kinetics depends on the adsorbate–adsorbent interaction and system condition and has been investigated for their suitability for application in water pollution control. Two vital evaluation elements for an adsorption process operation unit are the mechanism and the reaction rate. Solute uptake rate determines the residence time required for completing the adsorption reaction and can be enumerated from kinetic analysis. Numerous attempts were made in formulating a general expression to describe the kinetics of adsorption on solid surfaces for the liquid–solid adsorption system (Ho 2004). The adsorption rate is an important factor for a better choice of material to be used as an adsorbent; where the adsorbent should have a large adsorption capacity and a fast adsorption rate. Most of adsorption studies used pseudo-first-order and pseudo-second-order models to study the adsorption kinetics (Salleh et al. 2011).

In this work, the theories of adsorption kinetics are discussed under the following models:

1. First order model
2. Pseudo-first order model
3. Second order model
4. Pseudo-second order model
5. Elovich model.
6. Intra-particle diffusion model

First order model

A simplified first order rate equation used in representing it is as follows:

$$C_t = C_o e^{-k_1 t} \quad (2.5)$$

Equation 2.5 can be linearized to obtain equation 2.20.

$$\ln \frac{C_t}{C_o} = -K_1 t \quad (2.6)$$

C_t and C_o = solute concentration in (mg/l) at any time, t (s) and initial concentration in (mg/l) respectively, K_1 = first order rates constant (min^{-1}).

Hence, assuming first order kinetics is possible in the system, a plot of $\log C_t$ versus t of Equation (2.6) will give a linear graph of slope s , from which the constant K_1 and initial concentration C_o can be calculated using the relations $K_1/2.303$ and $\log C_o$ as slope and intercept respectively.

Pseudo-first order model

The first order rate equation was deduced to describe the kinetic process of a liquid – solid phase adsorption of oxalic acid and malonic acid onto charcoal. This is assumed to be the earliest model with regards to the adsorption rate based on the adsorption capacity.

$$\frac{dq}{dt} = K_{pt}(q_e - q_t) \quad (2.7)$$

Integrating eqn 2.21 using boundary conditions: $q_t = 0$ at $t = 0$ and $q_t = q_e$ at $t = t$, will yield

$$\ln q_e - \ln(q_e - q_t) = K_{p1}t \quad (2.8)$$

Rearranging the equation, it will give

$$\log(q_e - q_t) = \log q_e - \frac{k_{p1}}{2.303}(t) \quad (2.9)$$

If the Lagergren's first order kinetics works in the system, then a plot of $\log(q_e - q_t)$ against (t) will yield in a linear graph with $\frac{K_{p1}}{2.303}$ as gradient and $\log q_e$ as intercept. In order to differentiate the kinetic equations based on the adsorption capacity from solution concentration, Lagergren's first order rate has been called pseudo-first order.

Second order model

The equation in solution systems is represented as follows:

$$\frac{dc_t}{dt} = k_2 C_t^2 \quad (2.10)$$

Integrating equation (2.24), with the boundary conditions $C_t = 0$ at $t = 0$ and $C_t = C_t$ at $t = t$. It will give

$$\frac{l}{C_t} = k_2 t + \frac{1}{C_0} \quad (2.11)$$

Where C_0 and C_t (mg/l) are the equilibrium concentration of solute and concentration at anytime time, t. K_2 is the rate constant of second order model.

Pseudo-second-order model

Ho and Mckays (1999) explained the kinetic process of the adsorption of divalent metal ions onto peat. The driving force, $(q_e - q_t)$ is proportional to the available fraction of active sites. Then, it yields;

$$\frac{dq_t}{dt} = K_{p2}(q_e - q_t)^2 \quad (2.12)$$

re-arranging equation 2.26,

$$dq_t(q_e - q_t)^2 = K_{p2}dt \quad (2.13)$$

Integrating equation 2.27 with boundary conditions of $q_t = 0$ at $t = 0$ and $q_t = q_t$ at $t = t$, it yields;

$$\frac{1}{(q_e - q_t)} = \frac{1}{q_e} + K_{p2}t \quad (2.14)$$

Re-arranging equation 2.28 we will get

$$t/q_t = 1/K_{p2}q_e^2 + \frac{1}{q_e(t)} \quad (2.15)$$

Similarly, Ho's second-order rate equation has been called pseudo- second order rate equation to differentiate kinetic equations based on adsorption capacity from concentration. The pseudo second order kinetics model has been successfully used in several bio-sorption systems.

Elovich Model

This was developed by Zeldovich in 1934 to explain the rate of adsorption of carbon (ii) oxide (CO) on manganese dioxide. This is called the Elovich equation.

The equation is given below;

$$\frac{dq_t}{dt} = a e^{-\beta q_t} \quad (2.16)$$

Where q_t = amount of gas adsorbed at time (t).

t, a and β = the adsorption constant (g/mg) during experiment.

The equation shows that the rate decreases exponentially with rise in the quantity of gas being adsorbed. To simplify the elovich equation, Chien and Clayton, (1980) assumed $a\beta \gg t$ and by applying boundary condition at $q_t = 0$ at $t=0$ and $q_t = q_t$ at $t=t$, the equations becomes;

$$q_t = \frac{1}{\beta \ln(a\beta) - 1/\beta \ln(t)} \quad (2.17)$$

A plot of q_t versus $\ln t$ will give a linear relationship with $1/\beta$ as slope and $1/\beta \ln(a\beta)$ as slope and intercept respectively.

Intra-particle diffusion model

$$q_t = K_{id} t^{1/2} \quad (2.18)$$

In 1962, Weber Moris was the first to that in most adsorption processes, solute uptake varies directly as $t^{1/2}$ instead of with the constant time, t.

The logarithm form of the above equation is

$$\log q_t = \log K_{id} + 0.5 \log t \quad (2.19)$$

Where K_{id} = intra-particle diffusion rate constant. From equation (2.19), when $\log q_t$ is plotted against $0.5 \log t$, it will give a straight line with a positive intercept of $\log K_{id}$.

III. MATERIALS AND METHODS

The materials for this experiment include oil palm empty fruit bunch, obtained from Ihuokpara in Nkanu east local government area, Enugu State. Pharmaceutical wastewater, collected with a 20litres sterile gallon straight from the drug production company in Awka, Anambra state, Nigeria. The storage of the sample was done in a refrigerator at 3-8°C before analysis.

1) Reagents and Chemicals

The reagents include deionized water, normal hexane, wijs reagent, magnesium acetate, potassium iodide, sodium hydroxide, acetic acid. All the reagents are of the highest quality.

2) Instruments and Equipment

The various equipment used are electric grinder, electromagnetic sieve shaker (Model BA 200N), electronic digital weighing balance (Model PA 213), desiccator, muffle furnace (M1024), stainless steel beaker, hot plates, Brush, crucible, 20x150mm test tube, 1000ml Erlenmeyer flask, reflux condenser, 250 ml Erlenmeyer flask, pH meter (Hanna M921), Oven (Techmel M228 USA), petri-dish, oven, 100ml conical flask, heating mantles, magnetic stirrer, refrigerator, gallon, water bath, Atomic absorption spectrophotometer (Model FS240AA) and FTIR Spectroscopy (Model: M530).

Methods

Preparation, carbonization and oil palm empty palm fruit bunch activation

The samples were cleaned with deionized water and dried at 110 °C for 48 h to reduce the moisture content. The dried samples were then crushed and sieved to a range of 1–2mm. Subsequently, the samples were carbonized in a muffle furnace at 550°C at the rate of 20°C/min and held for 2 h. After carbonization, these samples were mixed with acetic acid (20%) in a stainless steel beaker in the weight ratio of 1:3. The mixture was stirred in a hot plate at 100°C for 1hr. Water was evaporated at 130°C for 4hrs, after which the dried mixture was heated at a rate of 10 °C/min to 800 °C, and the temperature was kept steady for one hour. The products were cooled to room temperature and washed with deionized water until the pH of the washing solution became neutral

CHARACTERIZATION OF THE RAW AND ACTIVATED OIL PALM EMPTY FRUIT BUNCH

Moisture content: This was determined according AOAC (1990) standard. A petri-dish was washed, dried in the oven and weighed, after which 1g of the sample was weighed into petri-dish. The petri-dish containing the sample was weighed w_1 . The petri-dish and sample were oven dried at 105°C for 2hr and weighed (w_2). The drying procedure was continuously repeated until a steady weight was obtained.

$$\% \text{moisture content} = \frac{w_1 - w_2}{\text{weight of sample}} \times 100\% \quad (3.1)$$

Where w_1 = weight of petri-dish and sample before drying

w_2 = weigh of petri-dish and sample after drying.

Ash content

The residue left after burning of sample is known as ash. It is generally composed of inorganic substances. The ash content was determined by weighing 2g of the sample in a crucible (w_1). The sample is spread with a brush. Then the crucible is kept inside a muffle furnace and the temperature is gradually raised up to 800°C. At 800°C the temperature is kept constant and the incineration of sample is completed by heating the sample for an hour at that temperature. After incineration, the crucible is allowed to cool and transferred to a desiccator. After cooling, the crucible is re-weighed (w_2). The percentage ash content is expressed in thus determined:

$$\text{Ash content} = \frac{w_2 - w_1}{\text{weight of sample}} \times 100\% \quad (3.2)$$

Volatile matter

Here 2g of sample is taken in a silica crucible with a porous silica cover. The weight of the silica crucible and sample is w_1 . The cover is used to avoid oxidation. The sample is then heated for 7 minutes at a constant temperature of 825°C inside a furnace. After heating, the crucible is cooled and transferred to a desiccator. After few minutes, the silica crucible is re-weighed (w_2). The difference between w_1 and w_2 gives the amount of apparent volatile matter in the sample.

$$\text{Apparent volatile matter} = \frac{w_2 - w_1}{\text{weight of sample}} \times 100\% \quad (3.3)$$

The actual volatile matter is the apparent volatile matter minus moisture content.

Actual volatile mater = Apparent volatile matter – moisture content

Fixed carbon:

This is defined as the free carbon content in a sample (that is in free state or uncombined with any element).

This is the difference between hundred and the sum of moisture, ash and volatile contents:

$$\text{Fixed carbon\%} = 100 - (\text{moisture\%} + \text{ash\%} + \% \text{volatile matter}) \quad (3.4)$$

Lignin content

The procedure according to Crampton and Mayrand (1978) was applied to measure the Lignin content as follows: 1g of sample weighed w_1 (initial sample weight), was placed in a 20 x 150mm test tube. 15ml of 72% was added and stirred for 1 minute until the sample is thoroughly wetted. The sample was transferred to a 1000ml Erlenmeyer flask and dilute to 500ml of deionized water. The flask, placed on the heating manifold, was boiled gently and refluxed for 4 hours in the reflux condenser. At the end of 4 hours, the condenser was rinsed with a small amount of deionized water before disassembling reflux apparatus.

The hydrolyzed solution was placed on the crucibles. The weight of collected filtrate was measured. The crucible and contents were dried at 105°C for 2 hours, after which it was cooled in the desiccators and recorded as w_2 . The crucible and contents were placed on the muffle furnace and ignited at 575°C for a minimum of 3 hours, or until all the carbon is eliminated; and then cooled in the desiccator and weighed as w_3

$$\% \text{ lignin} = \frac{W_2 - W_3}{W_1 - \frac{\text{total solid}}{100}} \times 100\% \quad (3.5)$$

Note: total solid = 100 – moisture content

Determination of Iodine content

The sample is weighed in into a 250 ml Erlenmeyer flask and 20 ml of glacial acetic acid is added. Thereafter, 25 ml of Wijs reagent and 10 ml of the magnesium acetate catalyst were added. The Erlenmeyer flask is closed with the stopper and kept dark for 8 to 10 minutes. At the end of the reaction duration, 10 ml of the Potassium iodide solution is added. The sample is diluted with 100 ml of deionized water and the excess of iodine is back titrated with $\text{Na}_2\text{S}_2\text{O}_3$ -Lösung (0.1 mol/L). A Blank value is measured.

$$\text{Iodine value} = \frac{(\text{blank-titre}) \times 1.269}{\text{weight of sample}} \quad (3.6)$$

Blank value = 27.7

Determination of pH

10g of the sample was weighed and placed in a beaker, after which 100ml of water was added. The whole solution was stirred thoroughly and allowed to stand for 1hr. Then the pH was read with a pH meter.

FTIR Analysis of the Raw and Activated Oil Palm Empty Fruit Bunch

Buck scientific M530 USA FTIR was used for the analysis. This instrument was equipped with a detector of deuterated triglycine sulphate and beam splitter of potassium bromide. The software of the Gram A1 was used to obtain the spectra and to manipulate them. An approximately of 1.0g of samples, 0.5ml of nujol was added, they were mixed properly and placed on the salt pellet. During measurement, FTIR spectra was obtained at frequency regions of 4000–600 cm^{-1} and co-added at 32 scans and at 4 cm^{-1} resolution. FTIR spectra were displayed as transmitter values.

SEM Analysis of the Raw and Activated Oil Palm Empty Fruit Bunch

The scanning electron microscopy (SEM) was performed to examine the physical structure change of samples using SEM model Phenom ProX, by phenom World Eindhoven, Netherlands. The sample, placed on double adhesive which was on a sample stub, was coated sputter coater by quorum technologies model Q150R, with 5nm of gold. Thereafter it was taken to the chamber of SEM machine where it was viewed via NaVCaM for focusing and little adjustment, it was then transferred to SEM mode, was focused and brightness contrasting was automatically adjusted, afterward the morphologies of different magnification was store in a USB stick.

AAS Instrumentation Study of the Pharmaceutical wastewater

The presence of heavy metals in the pharmaceutical wastewater was determined using AAS equipment. Lead and cadmium were among the prominent metals found at wavelength of 291.60 nm and 238.60 nm respectively. Other heavy metals found are Chromium, Zinc, Copper and Nickel at wavelengths of 360.50 nm , 214.22 nm , 325.65 nm and 234.10 nm respectively. However, this review is focused on lead and cadmium because of the obnoxious carcinogenicity resulting from the fact that their concentrations in the effluent are far above World Health Organization standards.

Adsorption Studies

The adsorption experiments were carried out in different batches by mixing 50ml of pharmaceutical wastewater with 0.1g of activated sample in a 200ml conical flask. The solution mixture was agitated at very high speed. The adsorbent particles were filtered off from the solution mixture, after which the filtrate was analyzed using AAS equipment to ascertain the amount of the target metals present after adsorption. The adsorption capacity of the activated oil palm bunch (amount of each metal adsorbed) and its efficiency of removing metals (Removal efficiency) were calculated using equations 3.7 and 3.10.

THE EFFECT OF PROCESS CONDITIONS ON THE ADSORPTION PROCESS

The Effect of Time: The effect of contact time on the rate at which the adsorbent adsorbs cadmium and lead ions was studied by mixing 50ml of the collected pharmaceutical wastewater with 0.1g or 100mg of the adsorbent, while keeping the temperature and pH steady at 45°C and 7 respectively for 30. The same procedure was used

45, 60, 75 and 90 minutes respectively. After vigorous mixing for each time interval, the solution was filtered using 0.45µm filter and the concentration of each metallic ion in the filtrate was ascertained using AAS study.

The Effect of Temperature: The study of the effects of temperature variation on the adsorption experiment was done by mixing 0.1g of the activated oil palm with 50ml of the wastewater solution, while keeping the stirring time and operating pH at 60mins and 7 respectively for 30°C. The reaction was repeated for 40°C, 50°C, 60°C and 70°C respectively; and in each case the solution was filtered using 0.45µm filter paper and the amount of metal ion in the filtrate was measured using AAS.

The Effect of Dosage: The determination of the effect of adsorbent dosage on the adsorption process was done by mixing 50ml of the wastewater solution with 0.1g at neutral pH, 60mins stirring time and 45°C operating temperature. Similar procedure was followed but with 0.2g, 0.3g, 0.4g and 0.5g adsorbent dosage respectively. In each case, a 0.45µm filter paper was used to filter the solution and AAS was used to measure the cadmium and lead ions in the filtrate.

Adsorption capacity and removal efficiency

The determination of the quantity of each metal removed by the adsorbent is done using the adsorption capacity mass balance equation (Gunay et al., 2007):

$$Q = \frac{V}{m} (C_0 - C_e) \quad (3.7)$$

Where Q = adsorption capacity in mg/g; V = volume of the solution in ml; m = mass of the adsorbent in g, C₀ and C_e = initial and equilibrium concentration each metal ion in mg/l. Thus after an instantaneous time, t, the adsorption capacity can be calculated as:

$$Q = \frac{V}{m} (C_0 - C_t) \quad (3.8)$$

Where C_t = metal ion concentration at that time. Other parameters have their usual meaning.

The removal efficiency of the metal is the percentage ratio of the amount of metal ion removed to the metal ion originally present.

$$\text{Removal efficiency (Re)} = \frac{\text{metal removed ion}}{\text{initial metal ion present}} \times 100\% \quad (3.9)$$

Thus after instantaneous time, t, equation 3.9 becomes:

$$\text{Removal efficiency (Re)} = \frac{C_0 - C_t}{C_0} \times 100\% \quad (3.10)$$

Adsorption Isotherms

The data obtained from the adsorption experiment was tested for fitness into Langmuir, Freundlich, Temkin and Dubinin-Radushkevich (R-D) isotherm models:

Langmuir Model

This model assumes monolayer adsorption at active sites of the adsorbent with no interaction between molecules of adsorbed metals (Hussein et al., 2019). According to Foo and Hameed (2010), Langmuir isotherm can be expressed as:

$$q_e = \frac{Q_{kl} C_e}{1 + k_l C_e} \quad (3.11)$$

Equation 5 when linearized becomes:

$$\frac{C_e}{q_e} = \frac{1}{Q_{kl}} + \frac{C_e}{Q} \quad (3.12)$$

Where q_e = equilibrium adsorption capacity, that is, the amount of metal adsorbed per unit mass of the adsorbent (mg/g), Q = highest unilayer adsorption capacity (mg/g), and k_l = Langmuir adsorption constant (L/mg), which relates to the adsorption energy (l/mg) respectively; C_e is the equilibrium concentration of the metal ion (mg/l), k_l and q are obtained from the intercept and slope of the graph of C_e/q_e against C_e.

The nature of the adsorption process is reflected in Langmuir model by a dimensionless quantity called separation factor R_L. Mathematically, it could be written as:

$$R_L = \frac{1}{1 + k_l C_0} \quad (3.13)$$

Where C₀ is the beginning concentration of the adsorbate.

Adsorption process is not reversible if the value of R_L = 0, it is favorable if 0 < R_L < 1, linear if R_L = 1 and unfavorable if R_L > 1 (Folasegun and Kovo, 2014, Anirudan and Radhakrishnan, 2008).

Freundlich Model

Hussein et al. (2019) opined that this isotherm considers multilayer adsorption on heterogeneous media. In linearized form, this model is presented thus (Freundlich, 1906):

$$\log q_e = \log k_f + \frac{1}{n} \log C_e \quad (3.14)$$

Where q_e = equilibrium adsorption capacity or the amount of metal adsorbed per unit mass of the adsorbent (mg/g), C_e is the equilibrium metal ion concentration (mg/l), k_f = Freundlich adsorption constant in mg/g; n = adsorption index reflecting the intensity of the adsorption process.

Temkin Model

This model considers the interaction between the adsorbents and the metal ions as a function of the surface coverage. Mathematically, Temkin's model is given as:

$$q_e = B \ln K_T + B \ln C_e \quad (3.15)$$

$$\text{Where } B = \frac{RT}{b} \quad (3.16)$$

Where K_T (L/mol) is Temkin binding constant at equilibrium relating to the maximum binding energy; B (RT/b) is a constant related to the adsorption heat, b (Jg/Lmol) is the adsorption constant, R (8.314 J/mol K) is the gas constant and T (K) is the absolute temperature.

Dubinin-Radushkevich (R-D) Model

In empirical form, this model is thus expressed:

$$\ln q_e = \ln q_n - \beta \varepsilon^2 \quad (3.17)$$

Where β is a coefficient related to the mean free energy of adsorption per mol of the metal ion (mol^2/J^2), q_n is the theoretical saturation capacity (mg/g) and ε is the Polanyi potential mathematically explained as:

$\varepsilon = RT \ln(1 + \frac{1}{C_e})$. C_e and q_e are the metal equilibrium concentration (mg/l) and equilibrium adsorption capacity (mg/g).

Adsorption Thermodynamics

Change in standard Gibbs free energy (ΔG), change in enthalpy (ΔH) and change in entropy (ΔS) are thermodynamic parameters used to further elucidate the metal ions adsorption by the activated oil palm empty fruit bunch. According to (Guerra et al., 2006), they can be calculated using the following formulas:

$$\Delta G = -RT \ln K \quad (3.18)$$

where K is the equilibrium constant obtained from each adsorption model, T the absolute temperature (K) and the universal gas constant $R = 8.314 \times 10^{-3} \text{ kJ K}^{-1} \text{ mol}^{-1}$. K could also be calculated from the relation:

$$K = \frac{C_a}{C_e} = \frac{C_0 - C_e}{C_e} \quad (3.19)$$

K , ΔG , ΔH and ΔS are related according to Van't Hoff correlation (Yildiz et al., 2004) as follows:

$$\ln K = \frac{\Delta G}{RT} = \frac{-\Delta H}{RT} + \frac{\Delta S}{R} \quad (3.20)$$

Thus when $\ln K$ is plotted against $\frac{1}{T}$, a straight line is obtained and the slope is equal to $\frac{-\Delta H}{R}$ while the intercept is equal to $\frac{\Delta S}{R}$. From here, the enthalpy and entropy are calculated accordingly.

Adsorption kinetics for removing heavy metals by the synthesized adsorbent

The rate at which the pores of the activated oil palm bunch adsorb the metallic ion impurities was used to carry out the kinetic studies. Here, 50ml of the collected pharmaceutical wastewater was combined with 0.1g of the adsorbent at constant temperature and neutral pH, for a contact time of 30, 45, 60, 75 and 90 minutes respectively. The decrease in concentration of the metals at the different contact times was used in obtaining the data for the kinetic studies, according to equation 3.8. The data obtained was checked for fitness by modeling into the following standard kinetic models in order to analyze the kinetic behavior of the adsorption of the cadmium and lead ions as well as the steps that control it:

First order kinetic model

First order kinetic model could be represented in linear form as $\ln C_t = \ln C_0 - K_1 t$; which can be further simplified as:

$$\ln \frac{C_t}{C_0} = -K_1 t \quad (3.21)$$

Where C_t = equilibrium adsorption capacity (mg/g), C_0 = initial metal concentration, t = stirring time (min) and K_1 = first order adsorption rate constant.

Pseudo-first order kinetic model

This kinetic model equation is represented in linear form as:

$$\ln (q_e - q_t) = \ln q_e - K_1 t \quad (3.22)$$

Where q_e = equilibrium adsorption capacity (mg/g), q_t = instantaneous adsorption capacity (mg/g), t = stirring time (min) and K_1 = pseudo-first order adsorption constant (min^{-1}).

The assumption of reversibility of the interaction between the adsorbent and adsorbate is the basis of the pseudo-first order kinetic model (Sen-Gupta and Bhattacharyya, 2011).

Pseudo 2nd order kinetic model

The linearized form of pseudo 2nd order model is presented in equation in equation 3.22:

$$\frac{t}{q_t} = \frac{1}{K_2 q_e^2} + \frac{t}{q_e} \quad (3.23)$$

Where q_e = equilibrium adsorption capacity (mg/g), q_t = instantaneous adsorption capacity (mg/g), t = stirring time in minutes and K_2 = pseudo-second order adsorption constant (g/mgmin).

Parameters q_e and K_2 are obtained from the slope and intercept of the plot of $\frac{t}{q_t}$ against t . Equation 3.23 shows that the adsorption rate varies directly as the square of the number of empty positions (Hussein et al., 2019).

Elovich kinetic model

Initially, this model was specifically designed for gas adsorption on solid surfaces. However, it also provides a good fit for adsorption in solid-liquid phase or solid-solid adsorption (Folasegun and Kovo, 2014). Therefore, this model studies adsorption in heterogeneous surfaces (Hussein et al., 2019). In straight line equation form, this model is expressed as(Wu et al., 2009):

$$q_t = \frac{1}{\beta} \ln(\alpha\beta) + \frac{1}{\beta} \ln(t) \tag{3.24}$$

Where α = initial adsorption rate constant (mg/min) at $t = 0$ while β is the extent of surface coverage and the activated energy.

Webber Morris kinetic model

Another name for this model is intra-particle diffusion kinetic model. In most cases, it is used in adsorption study (Das and Mondal, 2011). This model assumes that the intra-particle diffusion assay takes place as the solubized ions move from aqueous solutions to the adsorbent materials (Demiral and Gündüzoğlu, 2010). The model can be presented in linear form as follows:

$$q_t = K_d t^{1/2} + 1 \tag{3.25}$$

where K_d = intraparticle diffusion rate constant (mg/gmin^{1/2}), 1 = boundary layer effect mg/g, which is the intercept of the plot of q_t against $t^{1/2}$

Optimization studies

The purging of lead and cadmium ion impurities from pharmaceutical wastewater using activated oil palm fruit bunch is subject to certain reaction conditions, whose optimization will be done applying the Central Composite Rotatable Design (CCRD) of the Response Surface Methodology (RSM). The design was done with the aid of design expert (version 13); and it considered three independent factors of time, temperature, adsorbent dosage and one categorical factor of type of metal being removed. The response is the removal efficiency of the adsorbent. The rotatable composite design was built on full factorial design. Table 3.1 shows the null point, lower and upper points of each independent factor. The design matrix generated by the design expert, unveiling the number of runs and the conditions of experiments, is presented in Table 3.2. There are 40 design points comprising of 12 star-like points, 12 null points and 16 basic design points. The response of the optimization experiment (removal efficiency), calculated from equation 3.10, is based on the assumption that adsorbent removal efficiency increases as concentration of metal present decreases or as the adsorption capacity increases.

Table 3.1: Experimental Design

Factors	Symbols	Unit	-1	0	1
Time	A	mins	30	60	90
Temperature	B	°C	30	50	70
Dosage	C	G	0.1	0.3	0.5

Table 3.2: Design Matrix

Runs	Time (mins)	Temp (°C)	Dosage (g)	Type of metal
1	60	50	0.3	Cd
2	60	16.3641	0.3	Cd
3	60	50	0.3	Pb
4	30	70	0.1	Pb
5	30	30	0.5	Cd
6	9.54622	50	0.3	Cd
7	60	50	0.3	Cd
8	60	50	-0.0363586	Pb
9	60	50	0.3	Pb
10	60	50	0.636359	Cd
11	110.454	50	0.3	Pb
12	60	50	0.3	Cd
13	60	50	0.3	Pb
14	60	50	0.636359	Pb
15	30	30	0.5	Pb
16	30	30	0.1	Cd
17	60	50	0.3	Pb
18	90	30	0.5	Cd
19	9.54622	50	0.3	Pb
20	60	83.6359	0.3	Pb
21	60	50	-0.0363586	Cd
22	90	70	0.5	Cd
23	60	50	0.3	Cd
24	60	50	0.3	Cd
25	90	70	0.1	Cd

26	30	30	0.1	Pb
27	90	70	0.1	Pb
28	30	70	0.1	Cd
29	60	50	0.3	Cd
30	110.454	50	0.3	Cd
31	30	70	0.5	Pb
32	60	50	0.3	Pb
33	90	70	0.5	Pb
34	90	30	0.5	Pb
35	60	83.6359	0.3	Cd
36	30	70	0.5	Cd
37	60	50	0.3	Pb
38	90	30	0.1	Cd
39	90	30	0.1	Pb
40	60	16.3641	0.3	Pb

IV. RESULTS AND DISCUSSION

Characterization of the oil palm empty fruit bunch

Table 4.1: Proximate analysis of the raw and activated oil palm bunch

Parameters	Raw oil bunch	Activated oil bunch
Moisture content (%)	8.524	2.922
Volatile content	27.574	22.178
Ash content (%)	5.819	17.902
Fixed carbon	48.083	68.44
Lignin	6.159	20.257
Iodine content	24.074	44.267
pH	7.79	7.2

The nutritional value of the raw and activated oil palm empty fruit bunch, revealed by the proximate analysis carried out is tabulated in Table 4.1. The characteristics of raw oil palm include high fixed carbon, volatile materials, relatively high iodine content but comparatively moderate moisture content, lignin content and ash content. The pH value is within the alkaline range, though the alkalinity is small. The values above are within the confines of most literature. Furthermore, the high fixed carbon content portrayed the adsorbent efficacy of the palm fruit bunch (Thoe et al., 2019; Nick et al., 2021; Fazal and Rafique, 2013). These adsorbent characteristics increase after carbonization and activation with acetic acid; thus, the fixed carbon content, lignin content, ash content and iodine content increased while others decreased. According to Omar (2012), after thermal treatment of biomass, the volatile matter decreases thereby increasing the amount of surface pores as well as the fixed carbon content. Generally, iodine value of material is used to determine the degree of its unsaturation. Thus, the activated oil palm bunch has higher degree of unsaturation. This suggests a surge in chemical reactivity of the biomass after activation.

AAS Characterization Results

Table 4.2: AAS analysis of the pharmaceutical wastewater

Metals	Zn(ppm)	Ni(ppm)	Cd(ppm)	Pb(ppm)	Cu(ppm)	Cr(ppm)
Amount	0.698	0.0089	0.0235	0.2542	0.17	0.035
% Composition	58.68	0.748	1.97	21.37	14.29	2.942
WHO standard(ppm)	3-5	0.02	0.003	0.01	1-2	0.05

The Atomic Absorption Spectrometry (AAS) analysis was carried out to identify and determine the presence and amount of heavy metals present in the pharmaceutical wastewater sample. AAS is very sensitive and could detect minute amounts up to parts per billion. Table 4.1 showed at a glimpse that the AAS analysis detected the presence of six metals (Zinc, Nickel, Cadmium, Lead, Copper and Chromium) in parts per million. Cadmium and Lead are not the most prominent heavy metals as revealed by their percentage metal compositions; however, they are the only ones whose concentrations exceed the standard level according to the directives of the World Health Organization. Lead and cadmium have toxic effects even in minute concentrations. Researches have established that lead particles present in organic compounds poses serious danger and thus, they are grouped among cumulative poison. Acute poison symptom could result from exposure to lead over a sizeable amount of time. Health concerns such as mental retardation, kidney damage, stunted growth and skeletal anomaly could result from exposure to lead (Momodu and Anyakora, 2010). Cadmium has

in the material. There is a narrow band at about 1619 cm^{-1} , suggesting double bonds or aromatic compounds. Figure 4.2 is the spectrum of the oil after acid treatment. It has lesser peaks than Figure 4.1, suggesting the disappearance of certain compounds. This means that there are more vacant sites in the structure of original biomass and this could be attributed to the acid treatment. Also, the disappearance of certain compounds could also increase the level of unsaturation in the activated sample. Therefore, there is an increase in chemical activity of the activated biomass, resulting from increase in porosity and unsaturation due to chemical activation.

Morphology

Scanning Electron Microscopy (SEM) was done to reveal the morphology of raw and activated oil palm bunch.

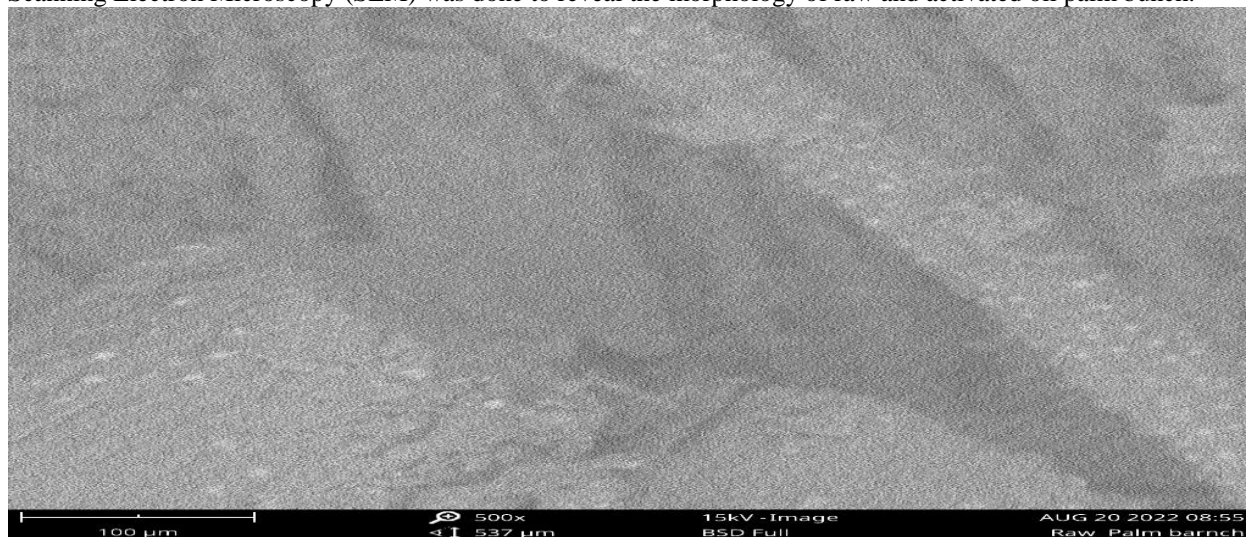


Plate 4.1a: SEM analysis of raw oil palm bunch



Plate 4.1b: SEM analysis of raw spent grain

Plates 4.1(a&b) are the morphological outlay of the raw or untreated oil palm bunch at $537\mu\text{m}$ and $269\mu\text{m}$ magnifications respectively. The micro structures appeared less porous. Keen glimpses of the plates' surfaces indicate they are smooth without much pores. Thus, this natural state of the biomass is unfit for efficient adsorption because the pores for molecular diffusion are not many.

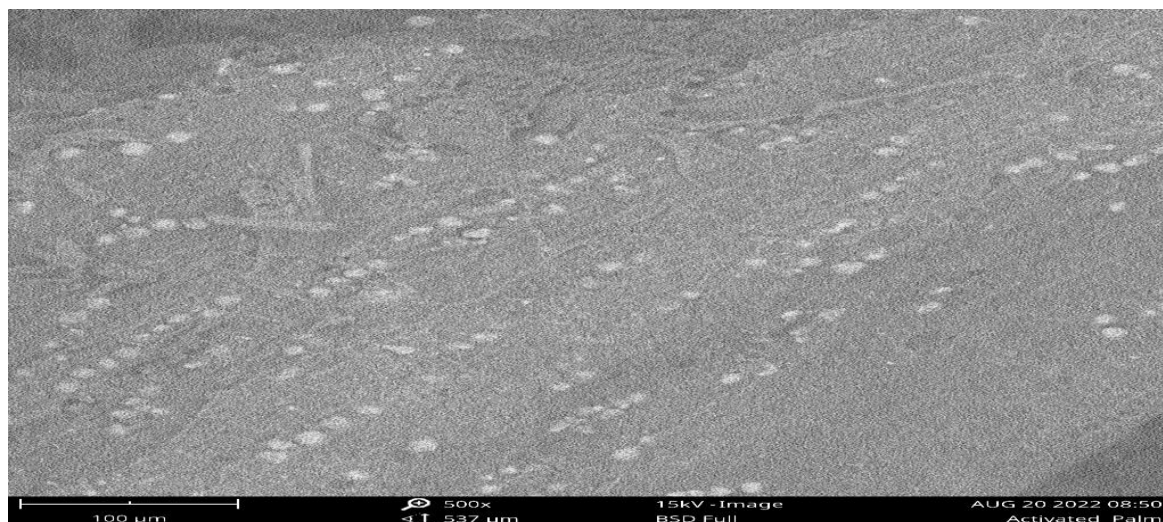


Plate 4.2a: SEM analysis of activated oil palm bunch

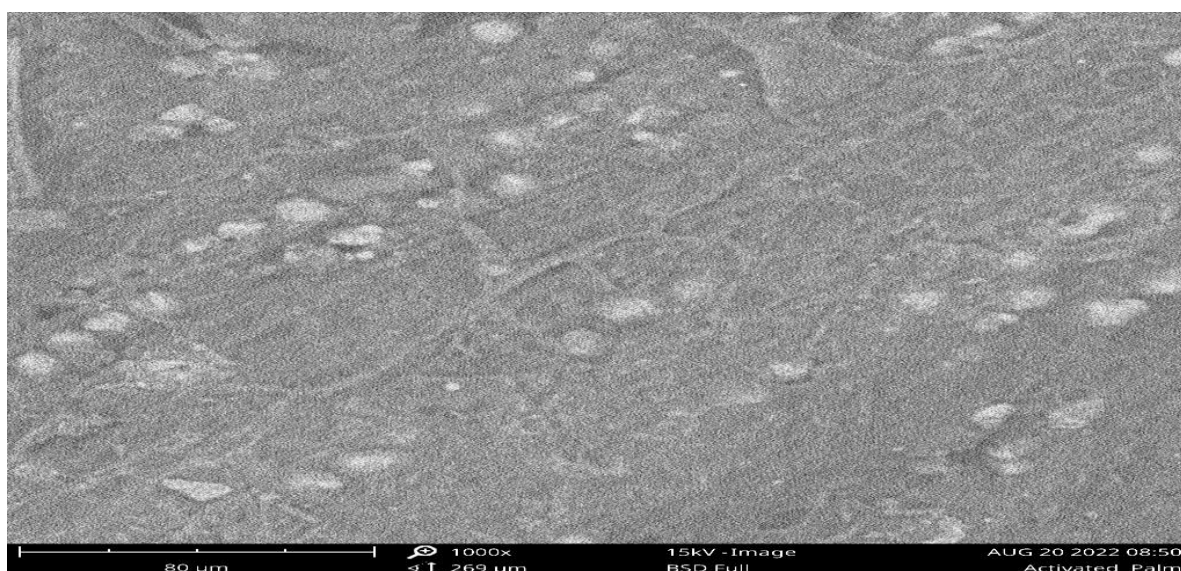


Plate 4.2b: SEM analysis of activated oil palm bunch

The morphological diagrams of the oil palm bunch after chemical activation are represented in Plates 4.2(a&b) at 537µm and 269µm magnifications respectively. The diagram portrayed high level of void spaces or pores in the activated sample. This increased in porosity is credited to the chemical activation of the waste biomass because during this process, some volatiles and inorganic particles were removed by the high temperature heat treatment or acid treatment. Because of the escapees, there are many vacant or void places for interstitial diffusion of the heavy molecules to take place when the pharmaceutical wastewaters are mixed with the activated samples.

Effect of Process Conditions on the Adsorption Process

The effects of varying process parameters such as stirring time, temperature and dosage of the synthesized adsorbent on the adsorption capacity and removal efficiency of the activated oil palm bunch were studied. The adsorption capacity and removal efficiency were calculated using equations 3.7 and 3.10 respectively.

Effect of stirring time on adsorption capacity and removal efficiency

The agitation time of the mixture of the wastewater sample and the activated biomass affects the rate at which metal impurities are being removed and also the adsorbent adsorption capacity. The minimum stirring time was 30mins while the maximum is 90mins. Intermittent checking was done to determine the effect of stirring time on adsorption capacity and removal efficiency and the result obtained is presented in Tables B1 and B2 in appendix B and in Figures 4.3 to 4.5.

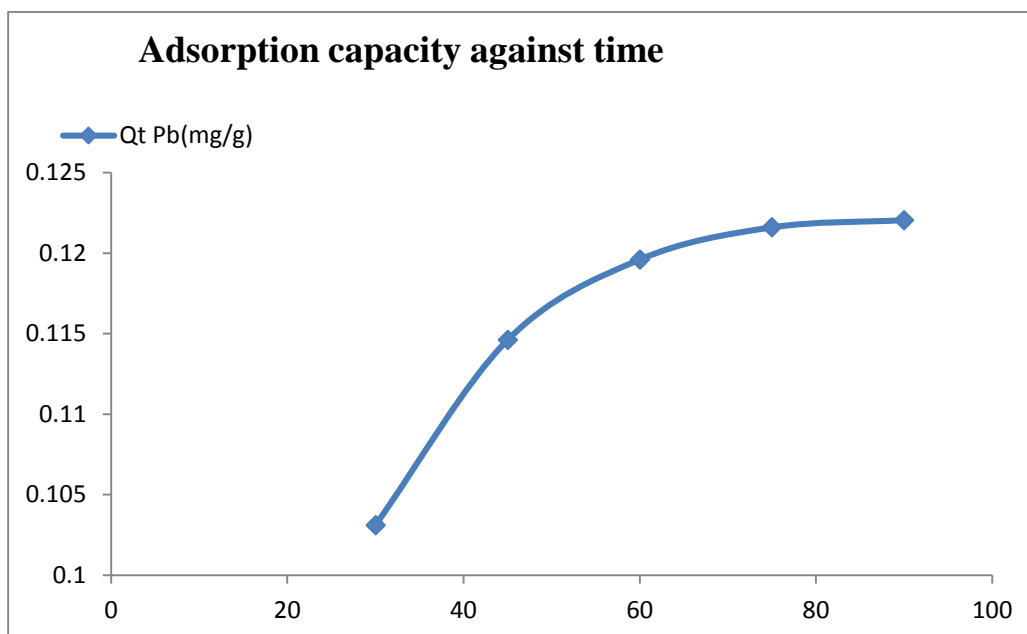


Fig 4.3: Adsorption capacity against stirring time during Lead removal

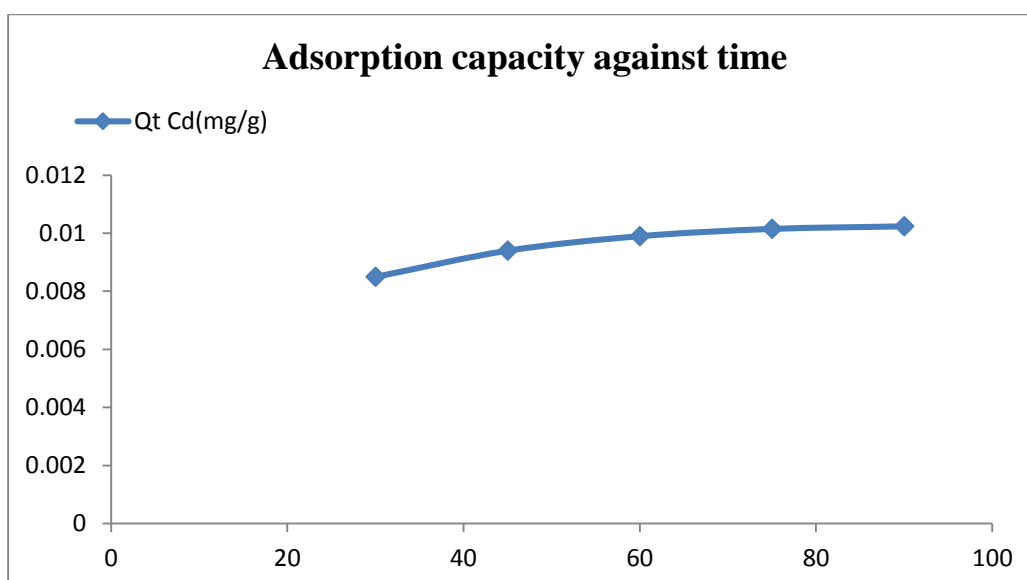


Fig 4.4: Adsorption capacity against stirring time during Cadmium removal

Time is a vital factor which affects the rate of adsorption of the metal by the activated adsorbent (Izinyon et al., 2016). Figures 4.4 and 4.5 revealed the relationship between stirring time and the metal uptake by the activated oil palm bunch. Generally, high stirring time increase the adsorption capacity of the adsorbent because enough time for thorough agitation of wastewater and activated sample mixture allows for more and more diffusion of the heavy metal particles into the micro-pores of the activated sample. This process continues until equilibrium is reached, when there are no more vacant spaces for the tiny impurities to occupy. In Figures 4.3 and 4.4, the fastest rate of impurities removal by the activated adsorbents is obtainable in the first 60mins. This is because high availability of active adsorption sites for the metal impurities to easily diffuse into and fill up. However, the rate of reaction slows down after this and by 75minutes and above, the rate curve becomes almost flat because equilibrium has been achieved since most of the void spaces have been filled up by the adsorbed metal impurities.

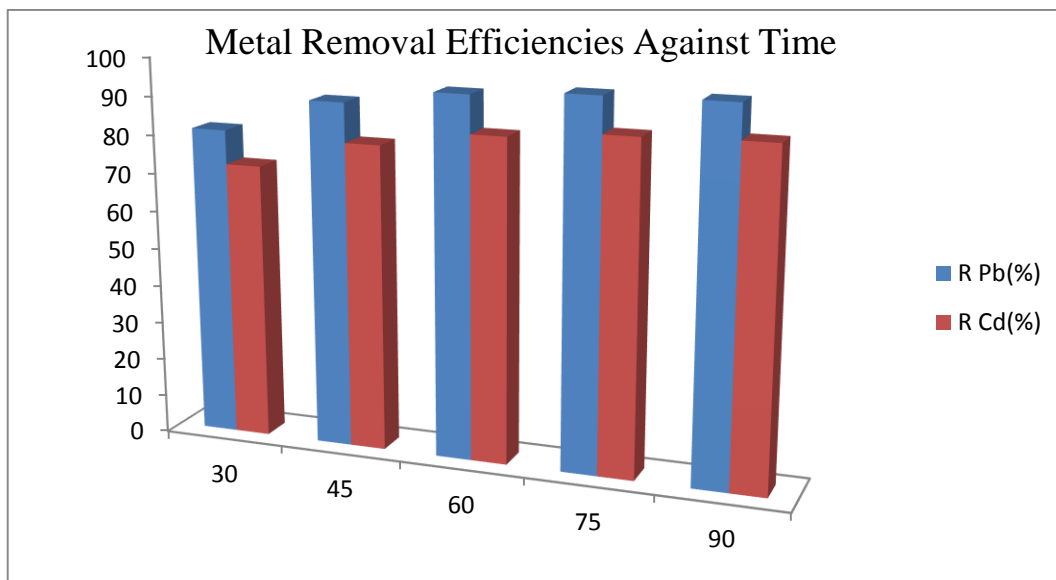


Fig 4.5: Lead and Cadmium removal efficiencies by the activated oil palm at different stirring time

Figure 4.5 presents quick comparison of the percentage of each metal removed by the adsorbent at the same conditions. The percentage lead removal is represented by the blue bar while the red bar represents the percentage cadmium removal. It is therefore easy to say that at any given condition, lead particles are more adsorbed than cadmium particles. This could be attributed to the higher initial concentration of lead ion.

Effect of temperature on adsorption capacity and removal efficiency

It is a known fact from elementary chemistry that high temperature increases the rate of most reactions because high temperatures increases the average kinetic energy of all the reacting particles, so that even the formerly less energetic ones are able to gain enough energy to surmount the reaction activation energy.

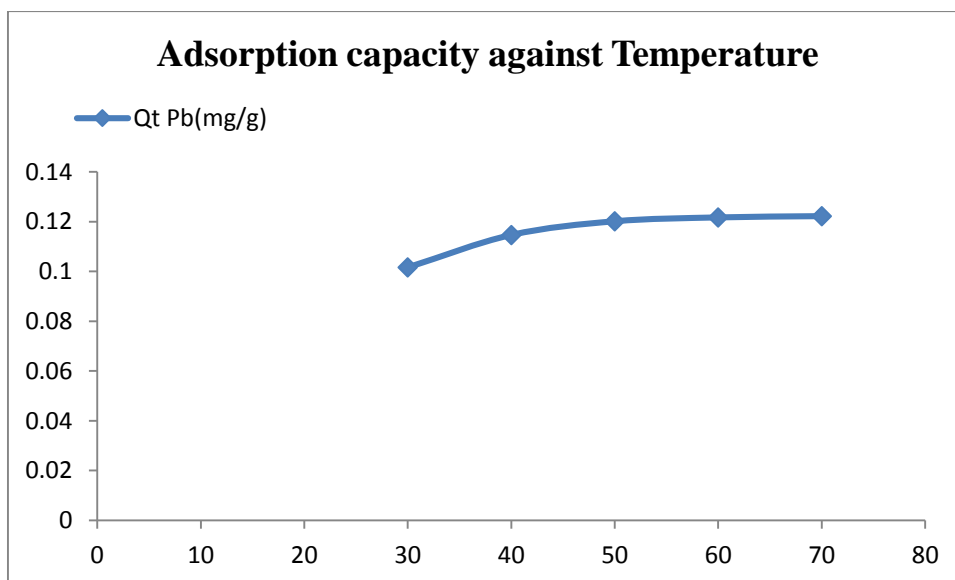


Fig 4.6: Adsorption capacity against temperature during lead removal

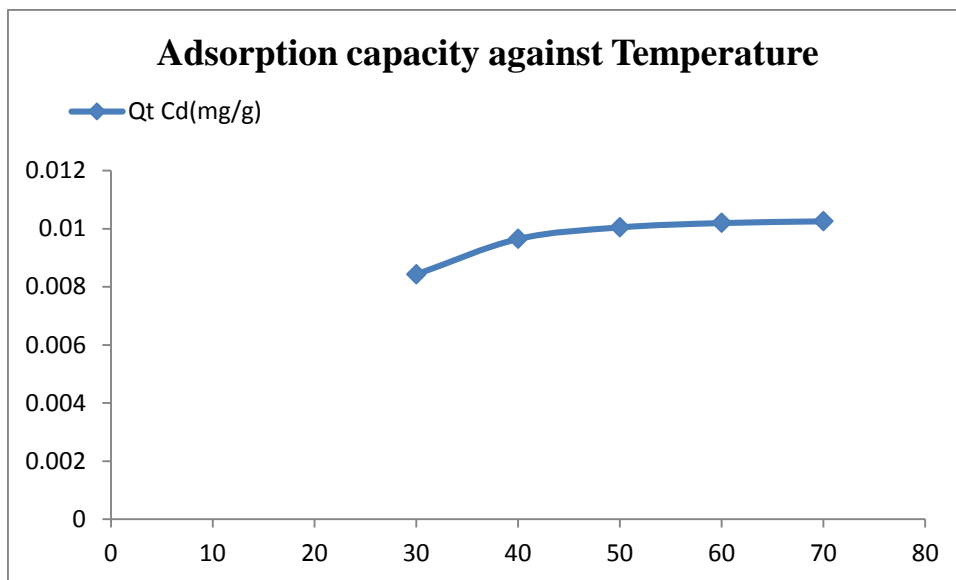


Fig 4.7: Adsorption capacity against temperature during Cadmium removal

As expected, Figures 4.6 and 4.7 buttressed the notion that reactions occur faster at high temperature. The ability of the adsorbent to adsorb the metal impurities increases with increase in temperature because high temperature increases the average kinetic energy of the adsorbent molecules so that they are able to circulate the entire body of the wastewater sample, thereby minimizing the average distance which the waste impurities travel being adsorbed; thus speeding up the adsorption process. Another important reason behind faster impurity removal at high temperature is because at high temperature, the metal impurities acquire enough energy to break away from the forces binding them, and therefore become free and more mobile, allowing for quicker diffusion to take place because the mobile metal ions will travel quickly to occupy all the vacant pores in the adsorbent material. This result conforms to the report of Asadu et al. (2022) in the removal of oil layer from surface water using plantain pseudo stem fiber. Mnasri-Ghnimi and Frini-Srasra (2019) opined that temperature increase is capable of increasing the pores of the adsorbent particles. According to Manohar et al. (2006), the rate of adsorption of the metallic ions is higher at high temperature because at high temperatures, the ion particles acquire sufficient energy to easily mingle with available sites of the adsorbent.

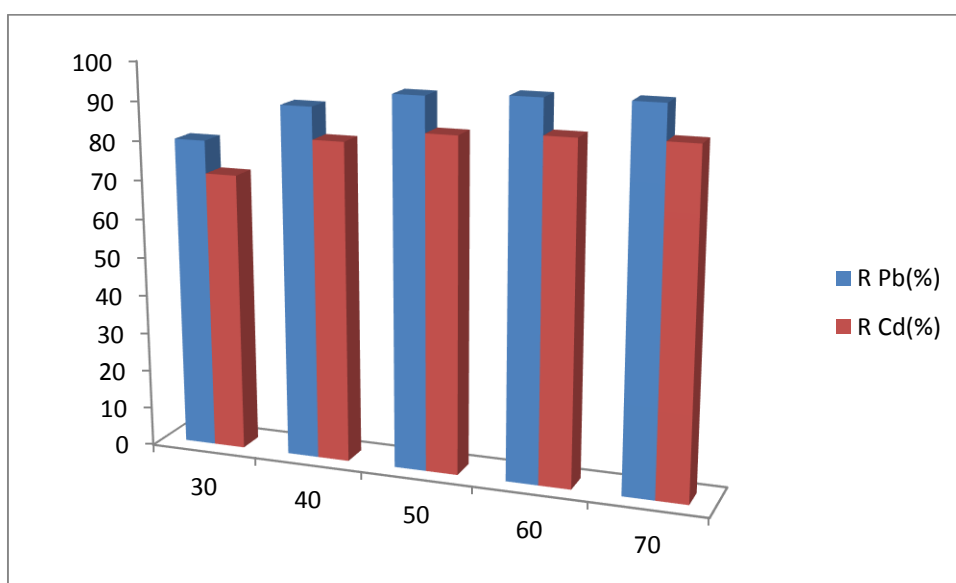


Fig 4.8: Lead and Cadmium removal efficiencies by the activated oil palm at different temperatures

Just as the case of varying stirring time, the percentage lead removal is more prominent at high temperature than percentage cadmium removal. Again, this could be attributed to the higher initial concentration of lead ion.

Effect of dosage on adsorption capacity and removal efficiency

The dosage of the prepared adsorbent affects its adsorption capacity. The effects of adsorption capacity is plotted in Figures 4.9 and 4.10 and presented in Tables B5 and B6 in the appendix B.

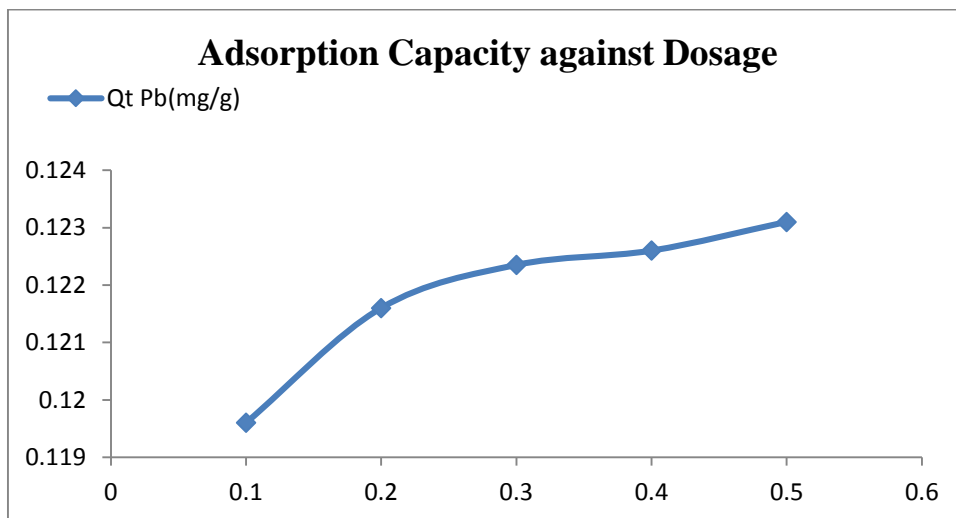


Fig 4.9: Adsorption capacity against dosage during lead removal

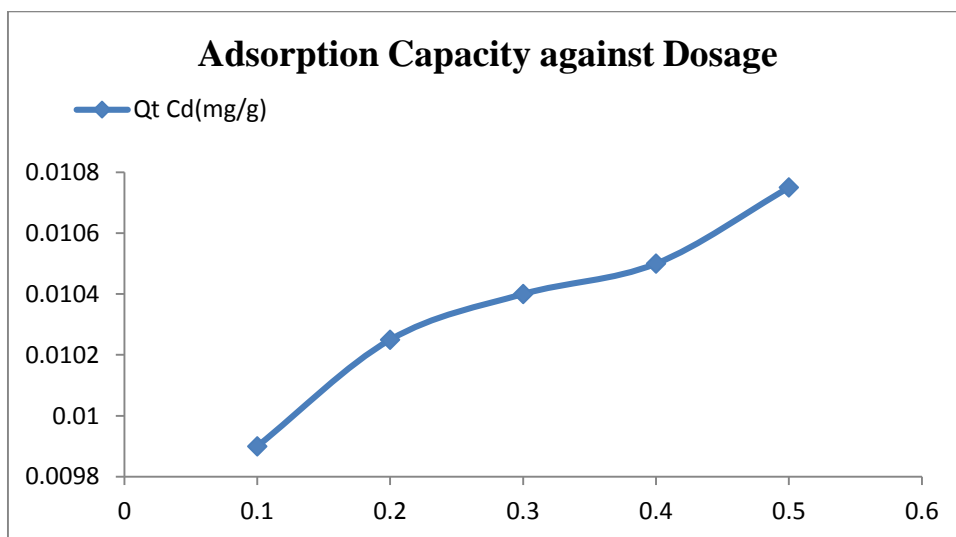


Fig 4.10: Adsorption capacity against dosage during Cadmium removal

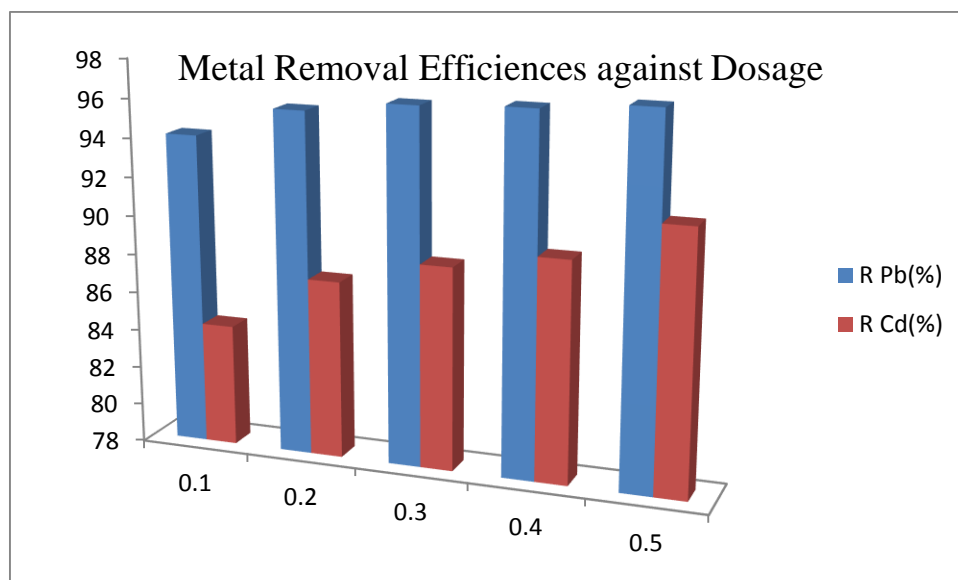


Fig 4.11: Lead and Cadmium removal efficiencies by the activated oil palm at different adsorbent dosages

The treatment of the wastewater is due to the deposition of the metal impurities on the vacant pores of the adsorbent. Since the number of available vacant pores increases with increase in the dosage of the activated adsorbents, it follows that the adsorption capacity of the adsorbent and hence its metal removal efficiency will also increase. In fact, among the three factors being discussed, adsorbent dosage is the most decisive factor in this pharmaceutical wastewater treatment by adsorption because the other factors are only there to facilitate the mixing of the adsorbent and the wastewater. This means that at the right adsorbent dosage, low temperature and insufficient stirring time, the adsorption could still take place but slowly and ineffectively. It is therefore important to maintain optimum temperature and agitation time to obtain the best result. The increase in adsorption of the adsorbate (lead and cadmium ions) at higher dosage of the activated biomass is simply due to the fact that at high dosage, there are sufficient spaces for the deposition of the impurity molecules into the boundary layer and inner pores of the activated oil palm bunch. Saeed et al. (2005) opined that higher dosage means higher active sites for metal adsorption to take place. Furthermore, Figure 4.11 follows similar trend with Figures 4.5 and 4.8 as it shows high percentage lead removal at for each dosage of the activated biomass.

ADSORPTION ISOTHERMS AND EQUILIBRIUM STUDY ANALYSIS

Rajeshkannan et al. (2011) reported that adsorption isotherms are fundamental to describing and designing any adsorption system. Isotherm models are also pertinent for ascertaining maximum adsorption capacity (Mnasri-Ghnimi and Frini-Srasra, 2019). Adsorption isotherms at a constant temperature also express the equilibrium relation between the amount of adsorbate adsorbed on the surface of the adsorbent and its concentration in the solution. The models investigated in this study include:

The Langmuir Isotherm Model:

According to Fadare et al. (2015), this model describes the quantitative forming of a one layer of the adsorbate on the exterior of the adsorbent, after which no further adsorption can take place. Equation (3.12) was used in plotting Langmuir model graph. The plots generated from the data in Tables C1 and C2 in the appendix C, are Figures 4.12 and 4.13 for lead and cadmium adsorption respectively.

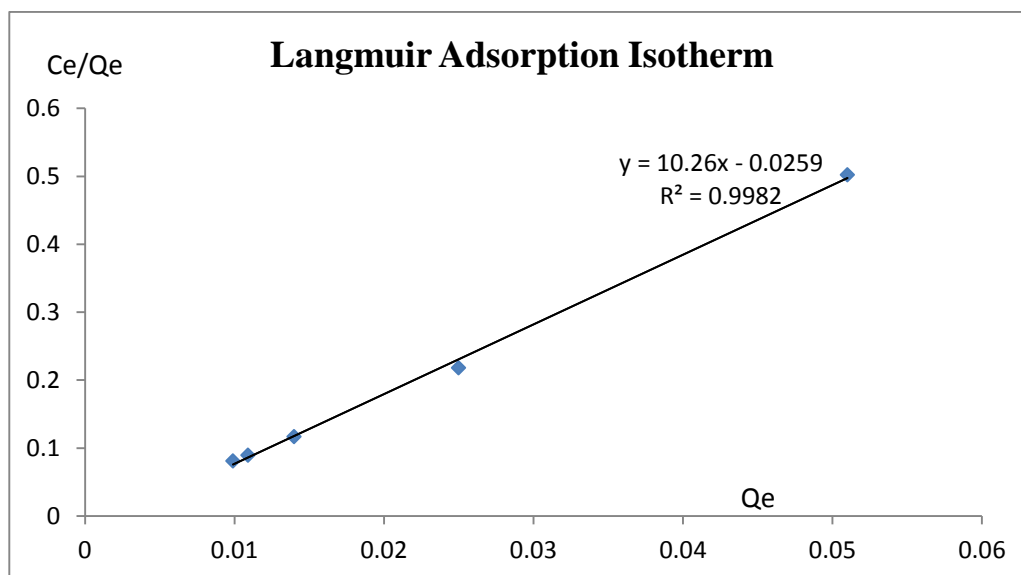


Fig 4.12: Langmuir isotherm for lead adsorption

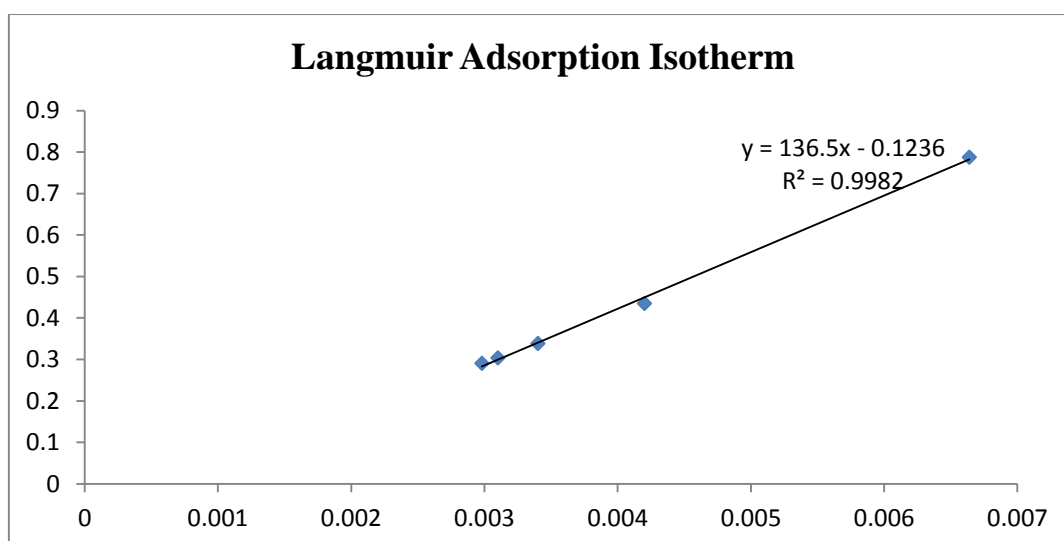


Fig 4.13: Langmuir isotherm for cadmium adsorption

Langmuir isotherm model provides almost a perfect fit for the removal of the target metallic ions as indicated by the linearity of Figures 4.12 and 4.13 and alignment of the data points. In addition, R^2 values of 0.9982 and 0.9982 for lead and cadmium ions removal are almost unity, buttressing the earlier assumption that this model is very suitable for the experiment. The values of the dimensionless quantity called separation factor (R_L), which was obtained from equation 3.13 are above zero but less than one, showing favorable adsorption. The positive values of Langmuir equilibrium constant (K_{ads}) could also be suggesting that the adsorption process is favourable. The sorption parameters, such as coefficient of regression (R^2), separation factor (R_L) and Langmuir constants (K_{ads}) are tabulated in Table 4.3.

The Freundlich Isotherm Model

Another model that has been proven to be an excellent fit by most literatures for adsorption of metal ions into activated biomass adsorbents is Freundlich adsorption isotherm. Freundlich adsorption model was plotted using the parameters from equation 3.14. The data for the plots are presented in Tables C3 and C4 in appendix C are the parameters from which Figures 4.14 and 4.15 were obtained. The Freundlich isotherm parameters, such as Freundlich constant, K_f , n and R^2 are presented in Table 4.3.

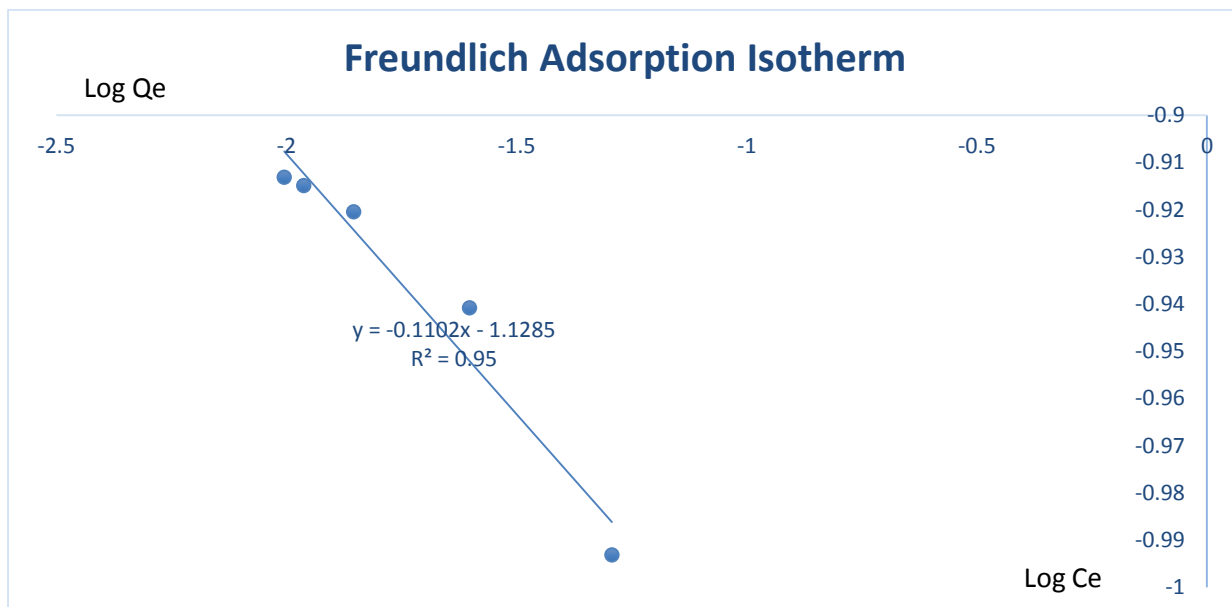


Fig 4.14: Freundlich isotherm for lead adsorption

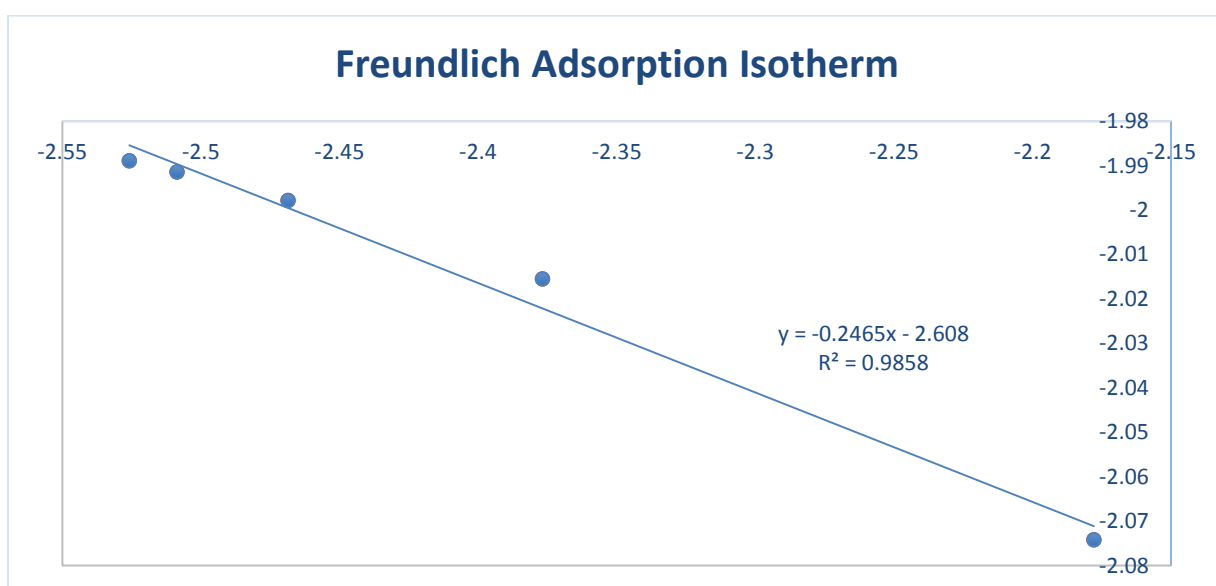


Fig 4.15: Freundlich isotherm for cadmium adsorption

A

According to Asadu et al. (2018), the constant K_f is a measure of the adsorption capacity while n is a measure of adsorption intensity or favourability. The constant n values of 9.1 and 4.1 (Table 4.3) for Freundlich model for lead and cadmium adsorption suggest that the adsorption is favourable since $1 < n < 10$ (Ladhe et al., 2011; Rabi & MunjurHasan, 2014). The closeness of the R^2 values (0.95 and 0.9858 for lead and cadmium adsorptions respectively) to 1 obviously indicated that Freundlich is also a good fit.

4.6.3 The Temkin Isotherm Model

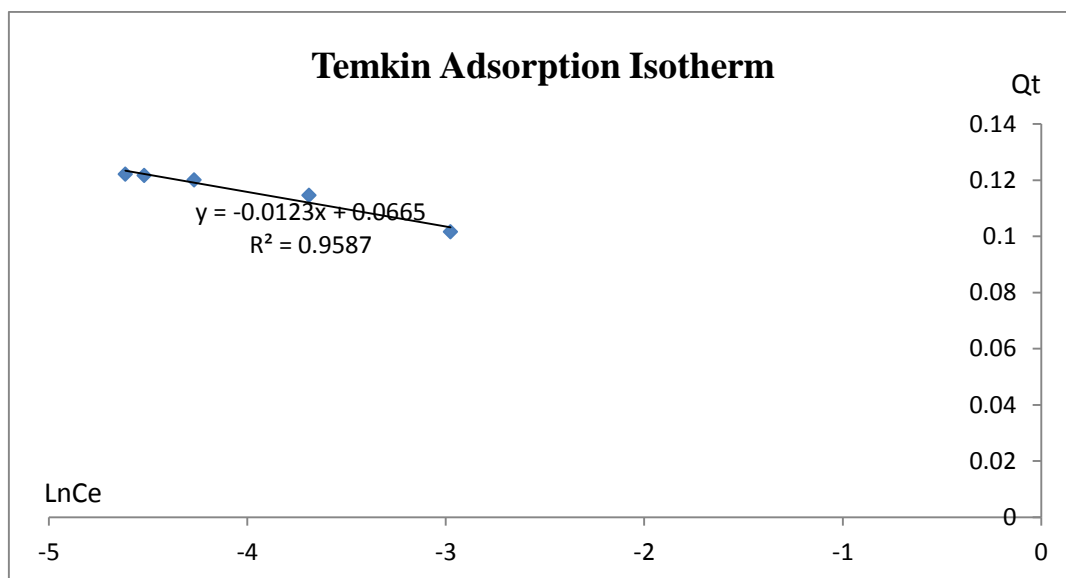


Fig 4.16: Temkin isotherm for lead adsorption

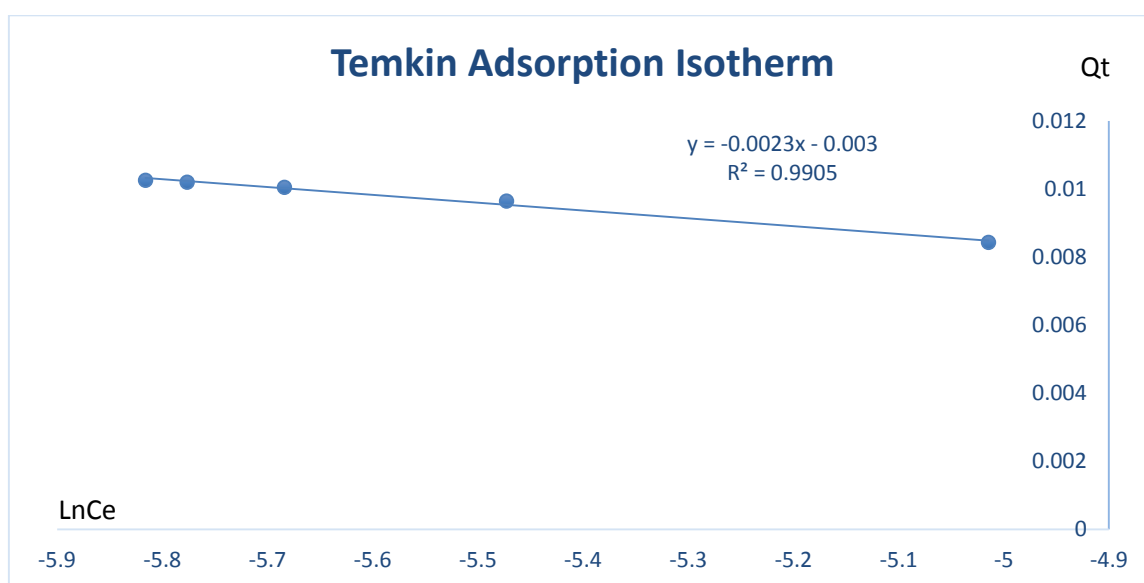


Fig 4.17: Temkin isotherm for cadmium adsorption

The plots obtained from Temkin model (equation 3.15) are Figures 4.16 and 4.17. Just like the Langmuir model, the linear alignment of points in Figures 4.16 and 4.17 suggests that Temkin's adsorption model is a perfect fit for this process. This is further supported by the R^2 values of 0.9587 and 0.9905.

The Dubinin-Radushkevich (R-D) Isotherm Model

Tables C7 and C8 in the appendix C present the data for obtaining this isotherm plots.

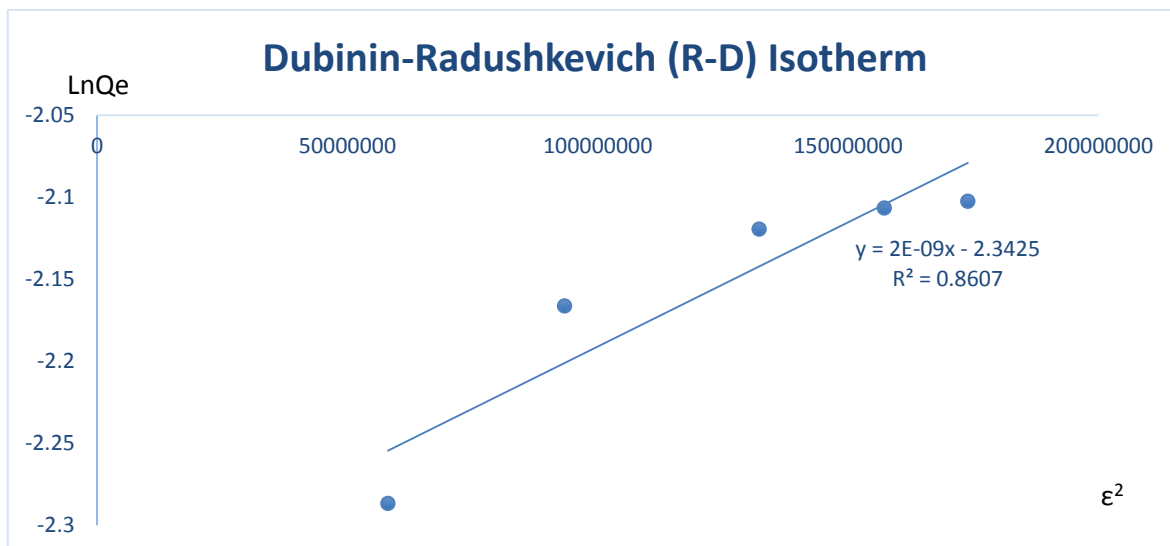


Fig 4.18: Dubinin-Radushkevich (R-D) isotherm for lead adsorption

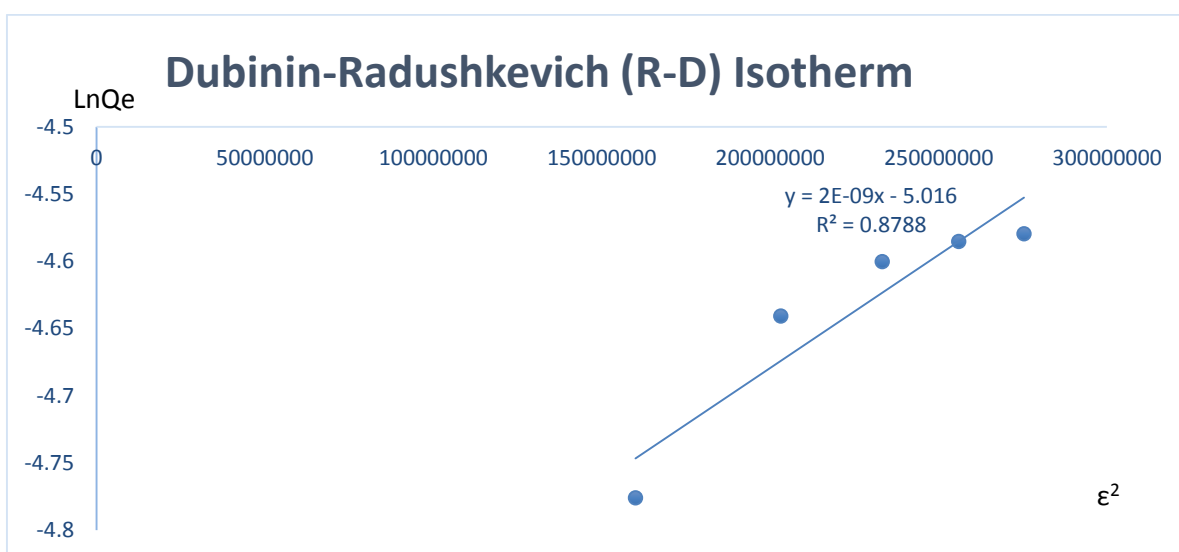


Fig 4.19: Dubinin-Radushkevich (R-D) isotherm for cadmium adsorption

R^2 values of 0.8607 and 0.8788 for Figures 4.18 and 4.19 suggest that this model is still ideal for describing the adsorption experiment. However, it is the least fitting model among the four models described in this study. This easily observed from the scattering of data in Figures 4.18 and 4.19 and the fact that the R^2 values are the lowest compared to other R^2 values in Table 4.3.

Table 4.3: Adsorption isotherm parameters

Langmuir Isotherms	Units	Pb	Cd
Kl	l/mg	396.1	1104.4
q_l	mg/g	0.0975	0.0073
R^2		0.9982	0.9982
R_L		0.01	0.04
Freundlich			
Kf		13.4	405.5
N		9.1	4.1
R^2		0.95	0.9858

Temkin			
B		-0.0123	-0.0023
K_T		222.9	3.7
R^2		0.9587	0.9905
Dubinin-Radushkevich			
B		-2×10^{-9}	-2×10^{-9}
q_m		0.096	0.0066
R^2		0.8607	0.8788

Table 4.3 suggests that the most fitting adsorption isotherm model for this experiment is Langmuir model followed closely by the Temkin model. This assumption is based on the R^2 values as Langmuir has the highest R^2 values while Dubinin-Radushkevich model has the least R^2 values.

Thermodynamics studies (Determination of the standard Gibb's free energy, enthalpy change and entropy change of the system)

The equilibrium constant (K) of the adsorption of the metal impurities was calculated using equation (3.19); and then used to determine the standard Gibb's energy using equation 3.18. K and ΔG values obtained are presented in Tables 4.4 and 4.5 for the removal of lead and cadmium impurities by the activated oil palm.

Table 4.4: Equilibrium constant and Gibb's free energy for Lead removal

Temp (K)	C_o (ppm)	C_i Pb(ppm)	K	ΔG
303	0.2542	0.048	4.295833333	3.672016153
313	0.2542	0.025	9.168	5.765926087
323	0.2542	0.015	15.94666667	7.436604393
333	0.2542	0.011	22.10909091	8.571437158
343	0.2542	0.0101	24.16831683	9.08279222

Table 4.5: Equilibrium constant and Gibb's free energy for Cadmium removal

Temp (K)	C_o (ppm)	C_e Cd(ppm)	K	ΔG
303	0.0235	0.0065	2.615384615	-2.42193125
313	0.0235	0.0047	4	-3.60752886
323	0.0235	0.0037	5.351351351	-4.50439022
333	0.0235	0.0032	6.34375	-5.11483545
343	0.0235	0.003	6.781456954	-5.45870507

ΔG values in Table 4.4 are all positive, suggesting that the adsorption of lead ions by the activated oil palm is endothermic (Asadu et al., 2019). Thus external energy is needed for swift diffusion of the lead molecules into the vacant pores of the adsorbent. In Table 4.5, ΔG values for cadmium adsorption by the adsorbent molecules are all negative. This implies that unlike the lead adsorption by the adsorbent, the removal of cadmium ions by the activated oil bunch is an exothermic process. Thus, less or no external energy is required for the adsorption of cadmium particles by the adsorbent molecules. The easy diffusion of the cadmium molecules into pores of the adsorbent could be attributed to their comparatively lower molecular weight and initial concentration in the wastewater sample.

The changes in enthalpy and entropy were calculated using the empirical relation between equilibrium constant (K), enthalpy change (ΔH) and change in entropy (ΔS) as contained in equation (3.20). Thus when $\ln K$ is plotted against $\frac{1}{T}$, a straight line plot is obtained, whose slope is equal to $\frac{-\Delta H}{R}$ and intercept is equal to $\frac{\Delta S}{R}$. The enthalpy change (ΔH) and entropy change (ΔS) calculated are presented in Table 4.6

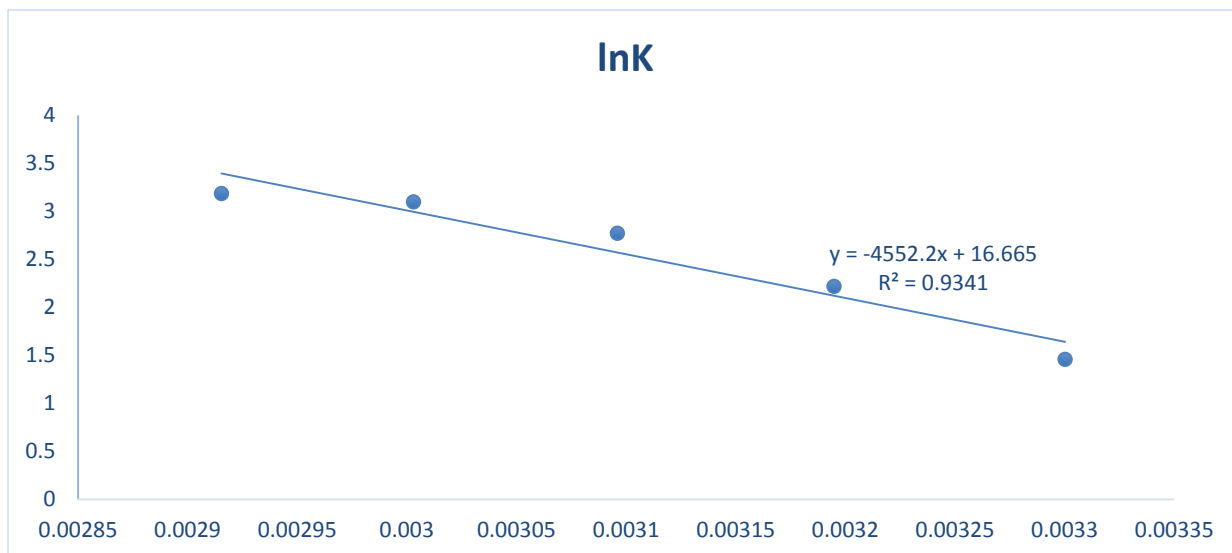


Fig 4.20: Thermodynamics plot for lead adsorption

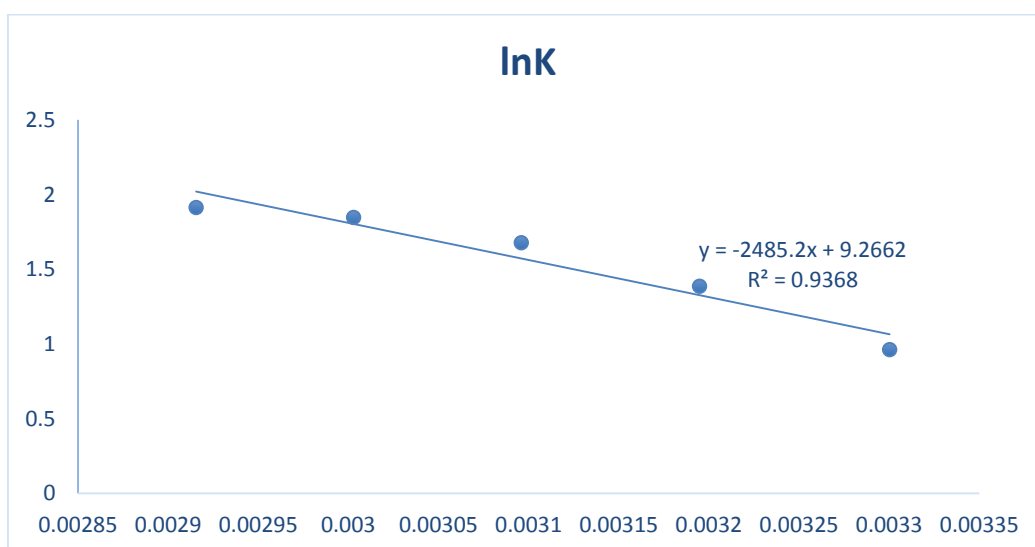


Fig 4.21: Thermodynamics plot for cadmium adsorption

Table 4.6: ΔH and ΔS for Lead and Cadmium adsorption

Parameters	Units	Pb	Cd
ΔH	(KJ/mol)	37.83	20.65
ΔS	(KJ/molK)	0.14	0.077
R^2		0.9341	0.9368

Adsorption Kinetics

Arivori et al. (2009) reported that adsorption kinetics is one of the decisive factors in determining the efficiency of the adsorption. Five adsorption kinetic models were employed in this work. The bases for plotting the kinetic models are equations 3.21 to 3.25. The kinetic plots are Figures 4.22 to 4.31 while the kinetic constants, R^2 values and other important parameters are tabulated in Table 4.7.

First Order Kinetic Model

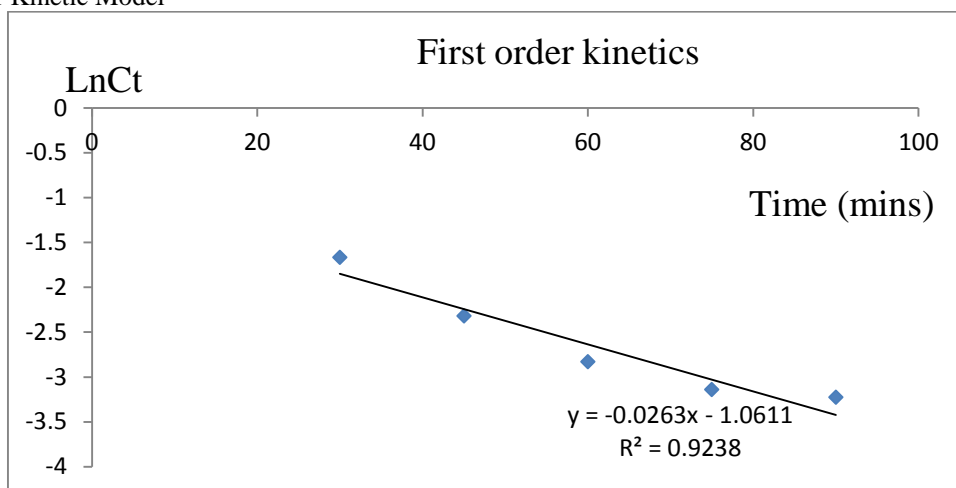


Figure 4.22: First order kinetics for lead adsorption

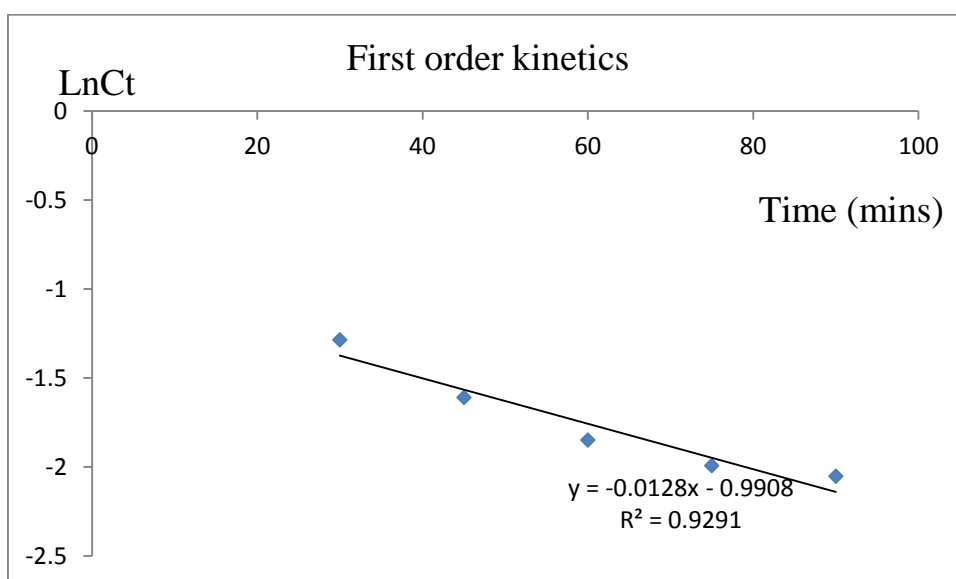


Figure 4.23: First order kinetics for cadmium adsorption

R^2 values of the model indicated that it is adequate for describing the kinetics of the removal of the metal impurities by the activated oil palm bunch. The first order rate constant was calculated from the slope of the plots and presented in Table 4.7

Pseudo-first Order Kinetic Model

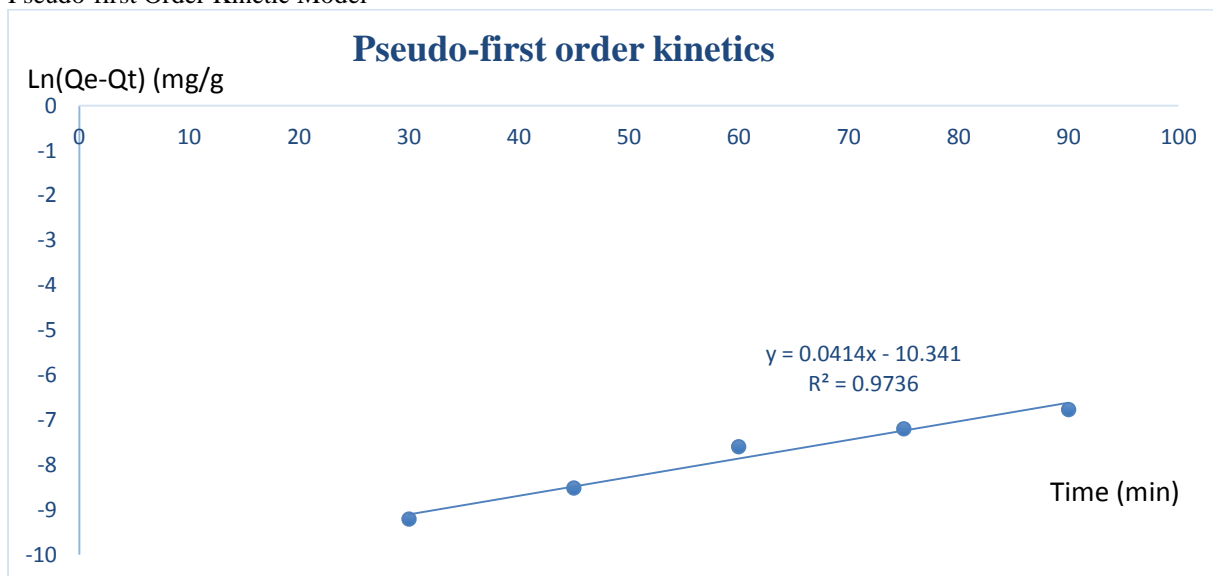


Figure 4.24: Pseudo-first order kinetics for lead adsorption

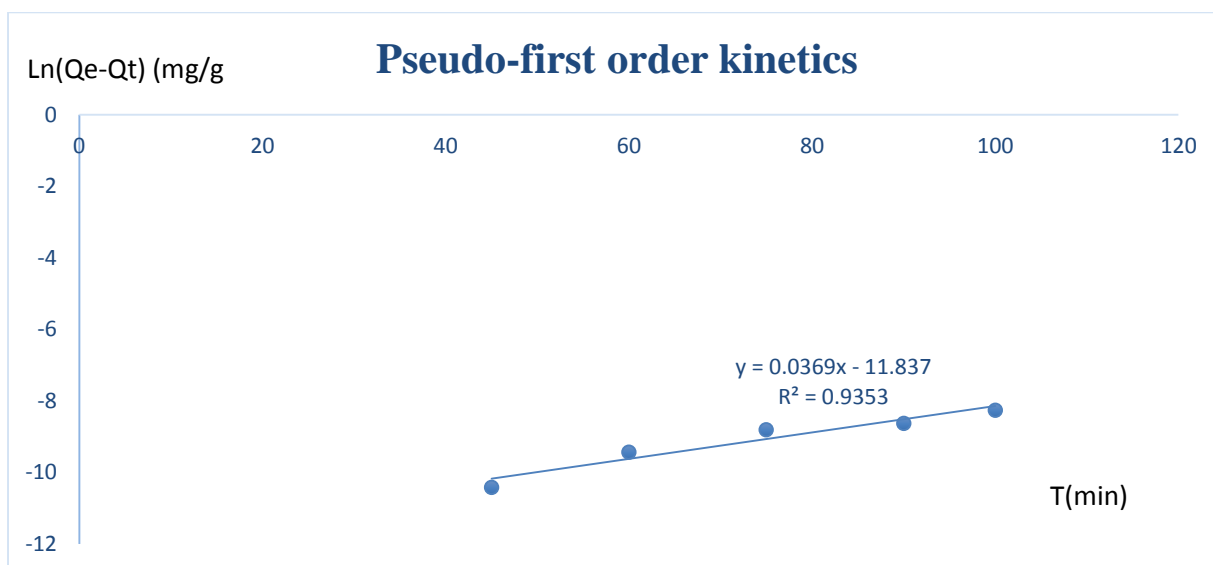


Figure 4.25: Pseudo-first order kinetics for cadmium adsorption

The parameters for plotting Figures 4.24 and 4.25 are tabulated in Tables D3 and D4. The closeness of the R^2 values of this kinetic model to one is a clear proof of its adequacy in describing the adsorption process. Thus, Pseudo-first order models are good for analyzing the adsorption kinetics of the adsorption process. The rate constants, the calculated equilibrium adsorption capacity and the measured equilibrium adsorption capacity at 303K for the adsorption process are presented in Table 4.6. The value of calculated adsorption capacity is much lower at the given temperature.

Pseudo-second Order Kinetic Model

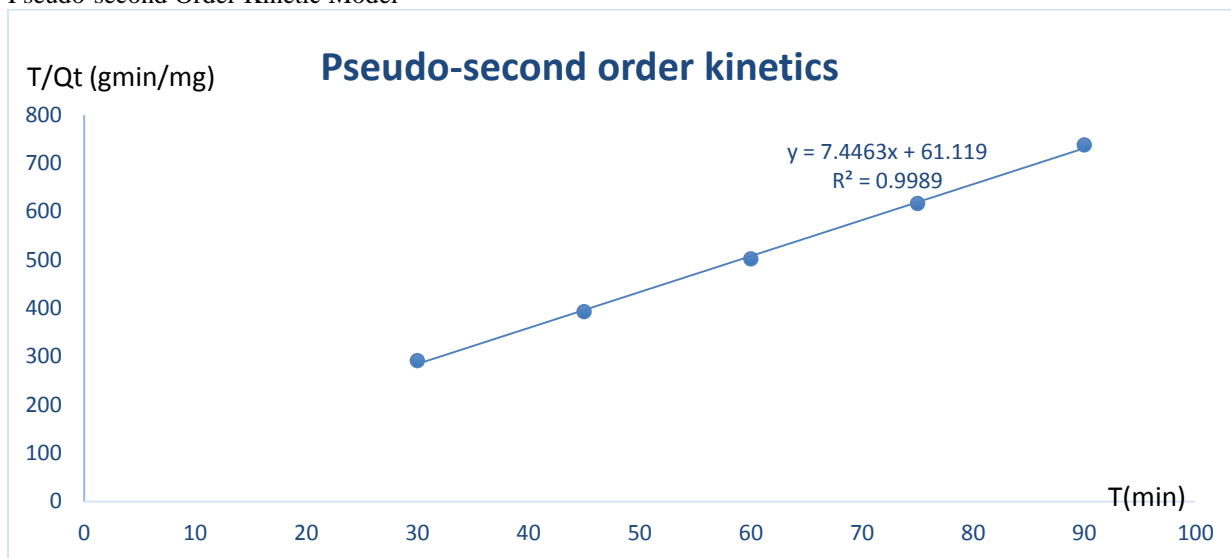


Figure 4.26: Pseudo-second order kinetics for lead adsorption

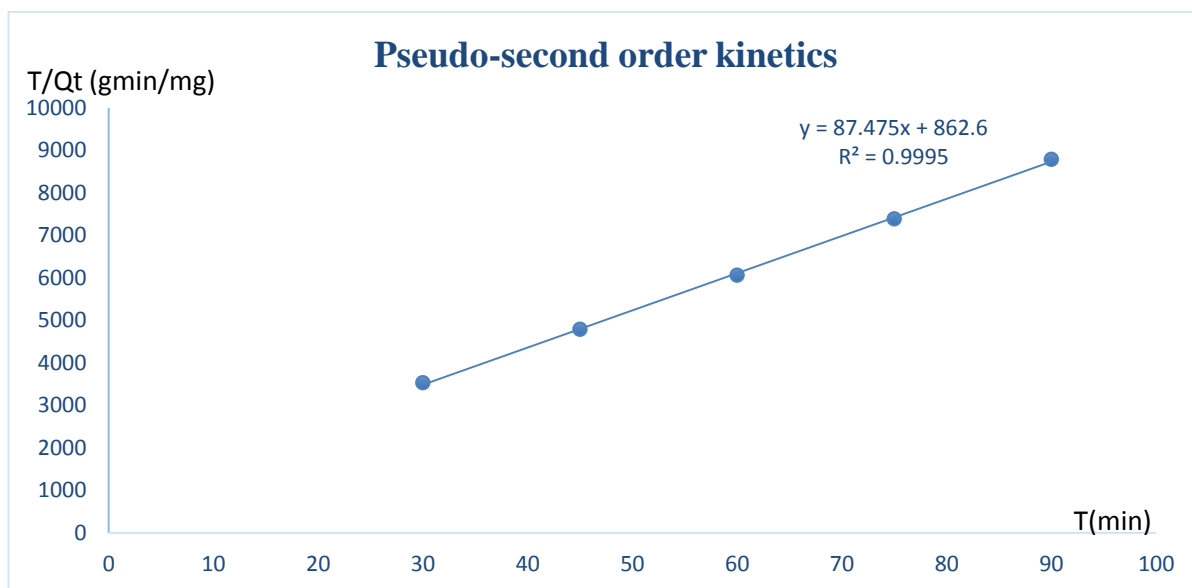


Figure 4.27: Pseudo-second order kinetics for cadmium adsorption

It is easy to assert that this model is the best fit for the sorption kinetics because of the perfect alignment of the data points and R^2 values high proximity to unity. This result agrees with the findings of Folasegun and Kovo (2014) and Izinyon et al., (2016). Since this model is based on chemisorption, this implies that chemisorption is actually the rate determining step. The calculated equilibrium adsorption capacity and the pseudo-second order rate constant are presented in Table 4.7.

Elovich Kinetic Model

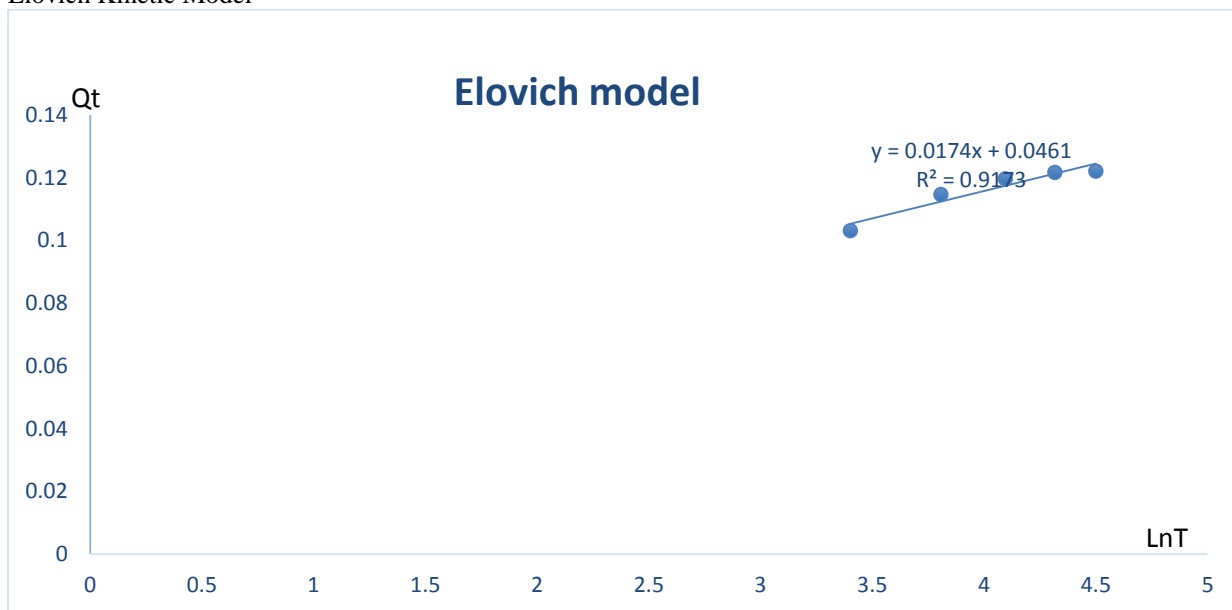


Figure 4.28: Elovich model for lead adsorption

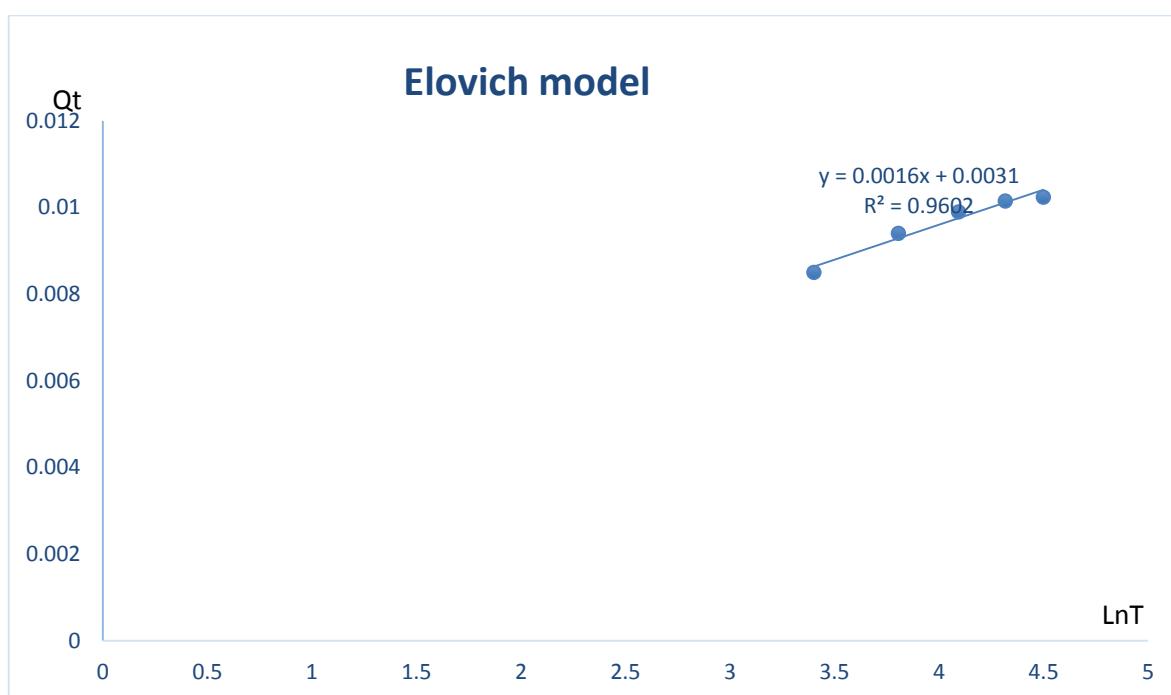


Figure 4.29: Elovich model for cadmium adsorption

R^2 values of Figures 4.28 and 4.29 suggest that this model could be used to describe the removal of the metal contaminants by the adsorbent. The fitness of this model in describing the adsorption experiment is also an indication that the adsorption process can occur in heterogeneous surface since this model is unique for describing adsorption studies in a heterogeneous surface (Hussein et al., 2019).

The initial adsorption rate α and the extent of coverage β , calculated from the slope and intercept respectively are also tabulated in Table 4.7.

Webber Morris Kinetic Model

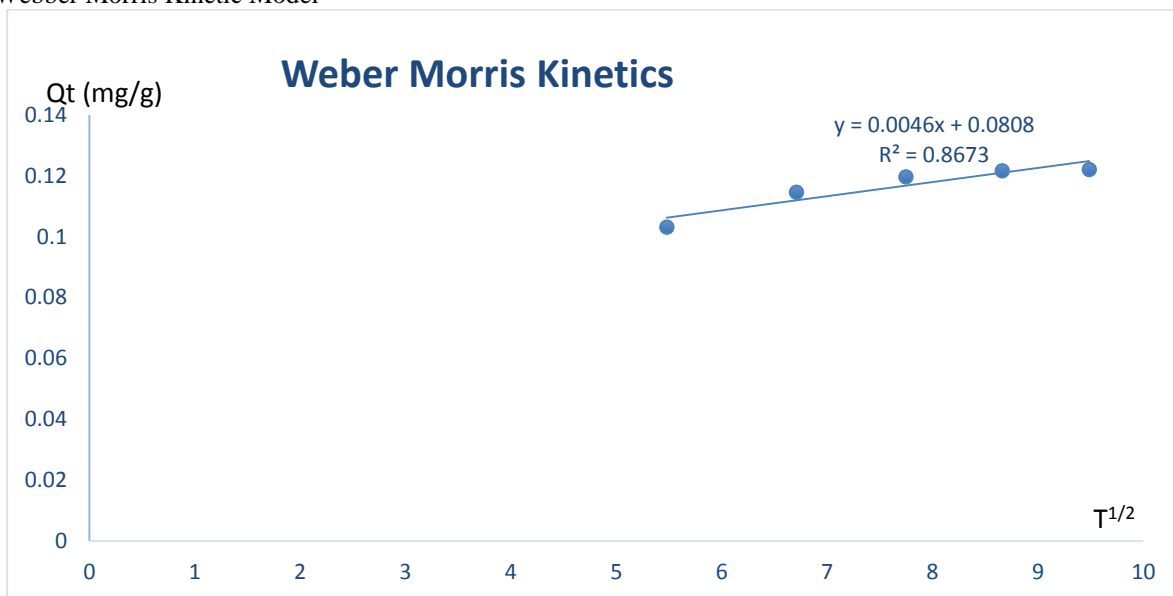


Figure 4.30: Weber Morris Kinetics for lead adsorption

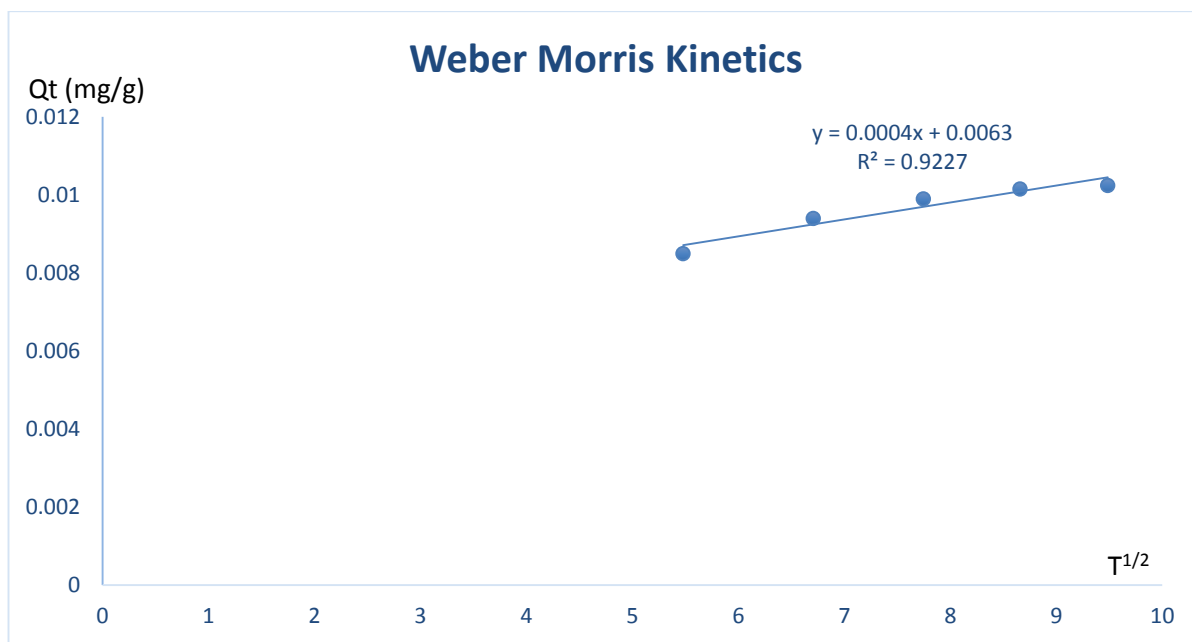


Figure 4.31: Weber Morris Kinetics for cadmium adsorption

This model is also called intra-particle diffusion kinetic model and according to Joseph et al. (2018), the adsorption capacity is linearly related to $t^{1/2}$ and not t . The regression coefficient (R^2) of this model also suggests its suitability.

Table 4.7: Adsorption kinetics parameters

	Units	Pb	Cd
First order			
K_1	Min ⁻¹	0.0263	0.0128
R^2		0.9238	0.9291
Pseudo-first order			
K_1	Min ⁻¹	0.0414	0.0369
Q_e calculated	mg/g	0.0000323	0.00000723
R^2		0.9736	0.9353

Pseudo-second order			
K ₂	g/mgmin	0.91	8.9
Q _e calculated	mg/g	0.134	0.0114
R ²		0.9989	0.9995
Elovich model			
A	Mg/gmin	0.246	0.0111
B	gmin/mg	57.5	625
R ²		0.9173	0.9602
Weber Morris model			
K _d	mg/gmin ^{1/2}	0.0046	0.0004
L	mg/g	0.0808	0.0063
R ²		0.8673	0.9227

Table 4.7 portrayed at a glance that pseudo-second order model is the R² values.

Process Optimization Using RSM

The response of the optimization experiment, calculated from equation 3.10 at each design point, was keyed into the design matrix (Table 4.8) for analysis.

Table 4.8: The Response of the CCRD for optimization experiment

Runs	Time (mins)	Temp (°C)	Dosage (g)	Type of metal	Response
1	60	50	0.3	Cd	75
2	60	16.3641	0.3	Cd	57
3	60	50	0.3	Pb	80
4	30	70	0.1	Pb	62
5	30	30	0.5	Cd	58
6	9.54622	50	0.3	Cd	58
7	60	50	0.3	Cd	75
8	60	50	-0.0363586	Pb	50
9	60	50	0.3	Pb	80
10	60	50	0.636359	Cd	88
11	110.454	50	0.3	Pb	93
12	60	50	0.3	Cd	75
13	60	50	0.3	Pb	80
14	60	50	0.636359	Pb	99
15	30	30	0.5	Pb	62
16	30	30	0.1	Cd	50
17	60	50	0.3	Pb	80
18	90	30	0.5	Cd	85
19	9.54622	50	0.3	Pb	62
20	60	83.6359	0.3	Pb	82
21	60	50	-0.0363586	Cd	50
22	90	70	0.5	Cd	94
23	60	50	0.3	Cd	75
24	60	50	0.3	Cd	75
25	90	70	0.1	Cd	55
26	30	30	0.1	Pb	55
27	90	70	0.1	Pb	60
28	30	70	0.1	Cd	60
29	60	50	0.3	Cd	75
30	110.454	50	0.3	Cd	81
31	30	70	0.5	Pb	85
32	60	50	0.3	Pb	80
33	90	70	0.5	Pb	99
34	90	30	0.5	Pb	90
35	60	83.6359	0.3	Cd	77
36	30	70	0.5	Cd	80
37	60	50	0.3	Pb	80
38	90	30	0.1	Cd	57
39	90	30	0.1	Pb	60
40	60	16.3641	0.3	Pb	60

The Response Model and Analysis of Variance (ANOVA)

Table 4.9: Model Summary Statistics

Source	Std. Dev.	R ²	Adjusted R ²	Predicted R ²	PRESS	
Linear	6.06	0.8344	0.8154	0.7778	1721.36	
2FI	4.55	0.9227	0.8960	0.8498	1163.46	
Quadratic	2.10	0.9851	0.9777	0.9511	379.18	Suggested
Cubic	1.63	0.9945	0.9866	0.8824	911.28	Aliased

Table 4.10: Quadratic model parameters

Std. Dev.	2.10	R ²	0.9851
Mean	72.47	Adjusted R ²	0.9777
C.V. %	2.90	Predicted R ²	0.9511
		Adeq Precision	43.9540

Metal removal

Color points by value of

Metal removal:

50  99

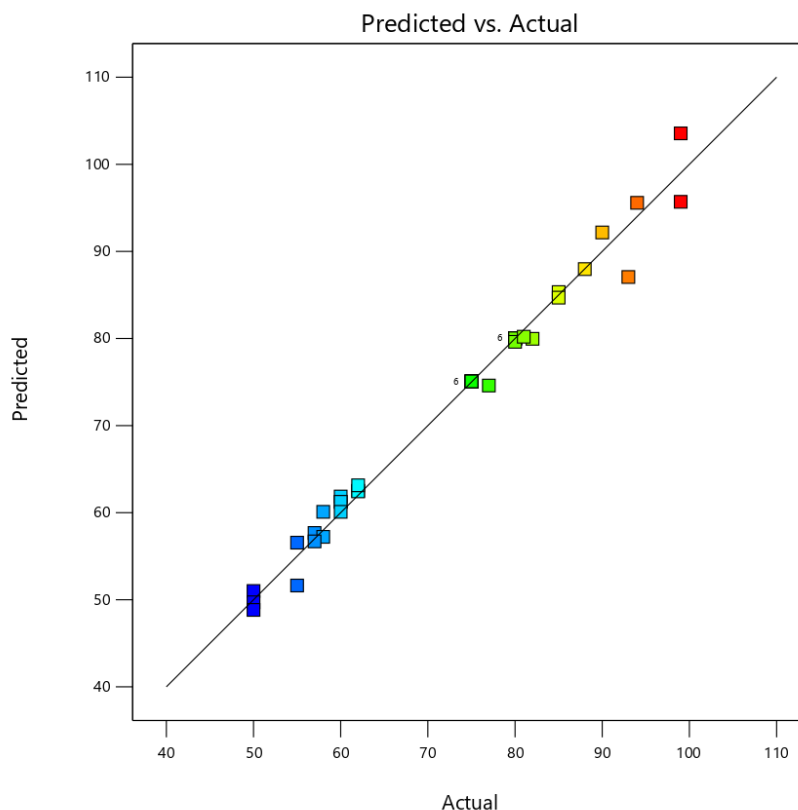


Fig 4.32: The predicted against the actual points

Table 4.9, generated by the design expert indicated that the suggested model is quadratic. This notion was supported by p-value of the model (Table 4.11), the model coefficient of determination (R^2) and the excellent alignment of the actual and predicted points (Figure 4.32). The p-value (<0.0001) of the quadratic model was less than the significance level of 0.05 (Table 4.11). The value of the coefficient of determination (R^2) was very close to unity (Table 4.10). The adequate precision value (43.9540) contained in Table 4.10 is used to determine signal to noise ratio, and it is acceptable because if it is above 4 (Taran and Aghale, 2015). Another important parameter in Table 4.10 is called coefficient of variation (C.V.) and it is the model's measure of the repeatability and reproducibility (Chen et al., 2011). The %C.V. value (2.9) of this model is reproducible because it is less than 10%, which is the standard for reproducibility (Chen et al., 2011).

Table 4.11: Analysis of Variance (ANOVA)

Source	Sum of Squares	df	Mean Square	F-value	p-value	
Model	7632.84	13	587.14	132.58	< 0.0001	Significant
A-Time	1170.67	1	1170.67	264.35	< 0.0001	
B-Temp	808.84	1	808.84	182.65	< 0.0001	
C-Dosage	4240.18	1	4240.18	957.49	< 0.0001	
D-Type of metal	245.02	1	245.02	55.33	< 0.0001	
AB	132.25	1	132.25	29.86	< 0.0001	
AC	380.25	1	380.25	85.87	< 0.0001	
AD	8.74	1	8.74	1.97	0.1718	

BC	144.00	1	144.00	32.52	< 0.0001	
BD	0.4142	1	0.4142	0.0935	0.7622	
CD	18.53	1	18.53	4.19	0.0510	
A ²	87.34	1	87.34	19.72	0.0001	
B ²	319.96	1	319.96	72.25	< 0.0001	
C ²	160.47	1	160.47	36.24	< 0.0001	
Residual	115.14	26	4.43			
Lack of Fit	115.14	16	7.20			
Pure Error	0.0000	10	0.0000			
Cor Total	7747.98	39				

The ANOVA shown in Table 4.11 elucidates easy understanding of the significance of the model and the process parameters in terms of their individual effects and relationship with each other, because it provides their F and P values at a glance. A parameter is deemed significant if its p-value is less than the 5% significance level. Shrivastvs et al. (2008) reported that the effect of the input variable(s) on the output(s) is more prominent when the model's P-value is very small. Thus, the single and quadratic effects of stirring time, temperature and adsorbent dosage, denoted with letters A, B, C as well as A², B² and C² are all significant. Similarly, their interactive effects with each other are also significant but their interactive effects with the categorical factor are insignificant.

The model has p-value far less (< 0.0001), which implies that the model accuracy is almost 100%.

Independent factors effects

Table 4.11 revealed that all the basic factors are significant owing to their very low p-value (<0.0001). The p-value is defined as the probability of the F-critical being greater than the F-values of the parameters. If the probability is more than the significance level, it means the parameter is not significant else the parameter is significant. Thus stirring time, temperature, dosage and even the categorical factor are significant factors which affect the removal efficiency of the activated oil palm bunch. The main factors effects are plotted as shown in Figures 4.33-4.38. The factors affect the removal of the metal contaminants positively. For each factor, there are two diagrams depicting the effect of that factor on the removal of the metals separately by the activated oil palm bunch. This is so because the type of metal being adsorbed by the adsorbent is a significant parameter.

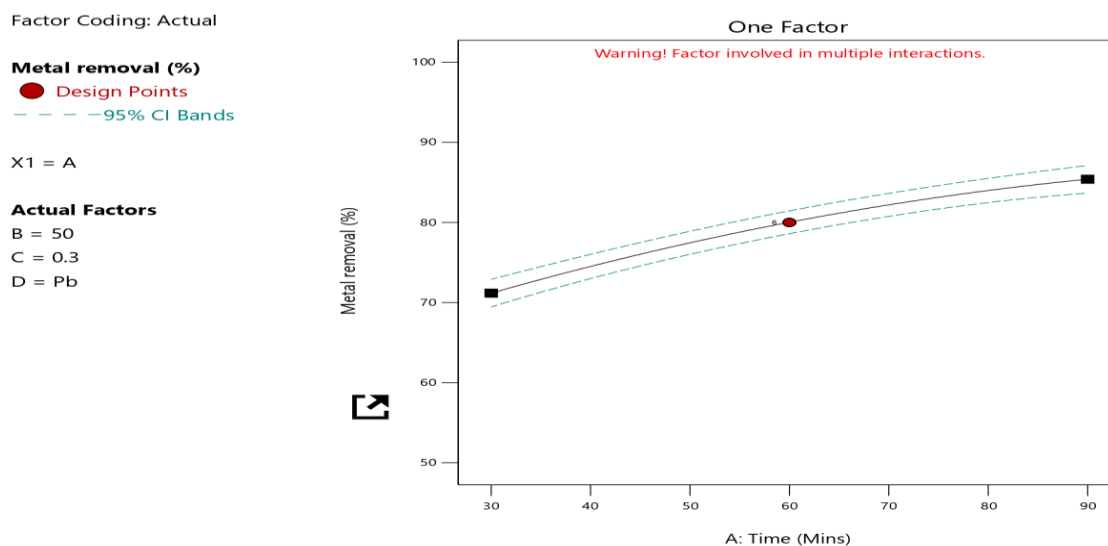


Figure 4.33: The main effect of time on percentage Lead removal

Factor Coding: Actual

Metal removal (%)
 ● Design Points
 - - - 95% CI Bands

X1 = A

Actual Factors

B = 50
 C = 0.3
 D = Cd

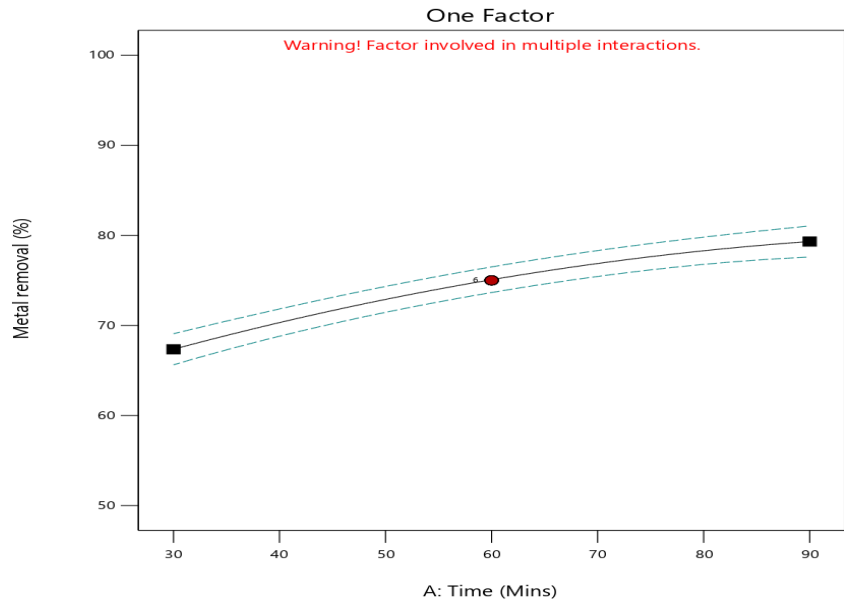


Figure 4.34: The main effect of time on percentage Cadmium removal

Factor Coding: Actual

Metal removal (%)
 ● Design Points
 - - - 95% CI Bands

X1 = B

Actual Factors

A = 60
 C = 0.3
 D = Pb

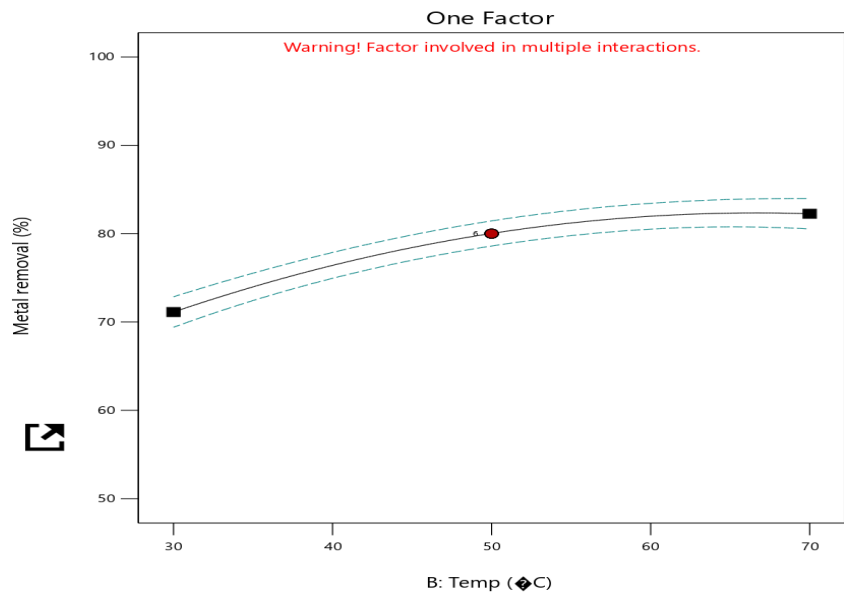


Figure 4.35: The main effect of temperature on percentage Lead removal

Factor Coding: Actual

Metal removal (%)
 ● Design Points
 - - - 95% CI Bands

X1 = B

Actual Factors

A = 60
 C = 0.3
 D = Cd

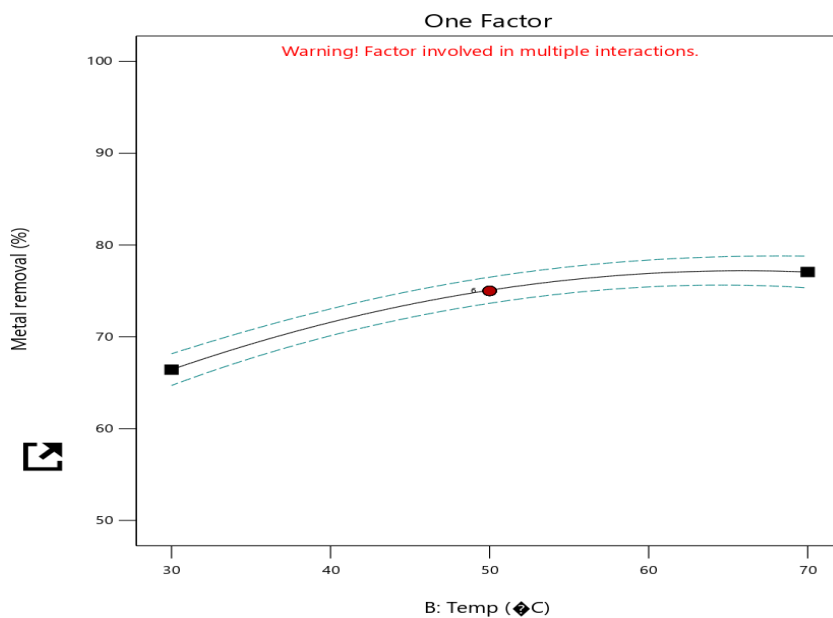


Figure 4.36: The main effect of temperature on percentage Cadmium removal

Factor Coding: Actual

Metal removal (%)
 ● Design Points
 - - - 95% CI Bands

X1 = C

Actual Factors

A = 60
 B = 50
 D = Pb

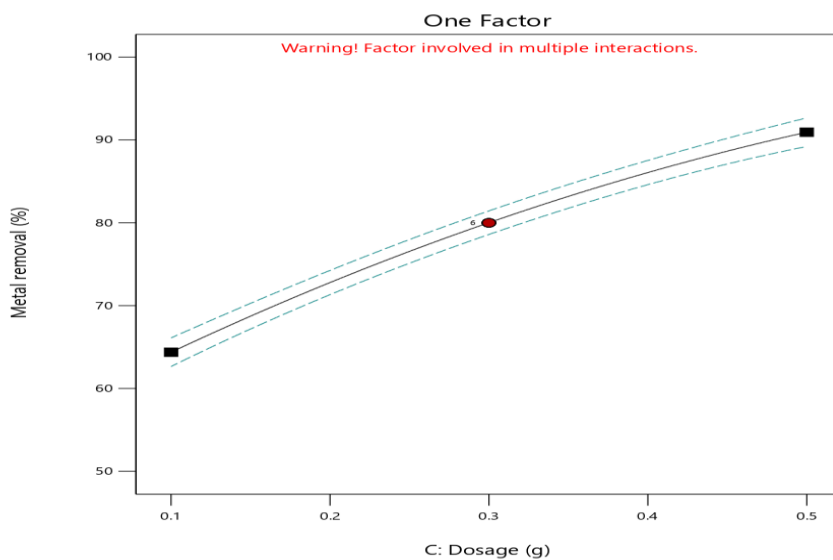


Figure 4.37: The main effect of adsorbent dosage on percentage Lead removal

Factor Coding: Actual

Metal removal (%)
 ● Design Points
 - - - 95% CI Bands

X1 = C

Actual Factors

A = 60
 B = 50
 D = Cd

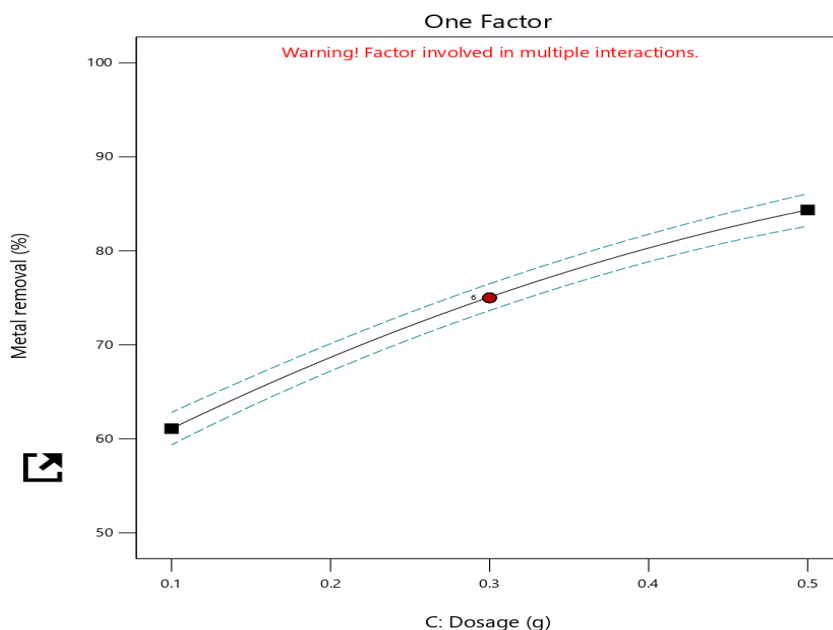


Figure 4.38: The main effect of adsorbent dosage on percentage Cadmium removal

Interactive effects and the 3D diagrams

The fact that optimization tries to relate the process parameters (independent factors) with the response (dependent factor) proves its interactive quality (Agu et al., 2015). As said earlier, the interactive effects of the factors (AB, AC and BC) are very significant. The interactive effects are plotted as three dimensional diagrams in Figures 4.39 to 4.44.

Factor Coding: Actual

Metal removal (%)
 ● Design Points
 50 99

X1 = A
 X2 = B

Actual Factors

C = 0.3
 D = Pb

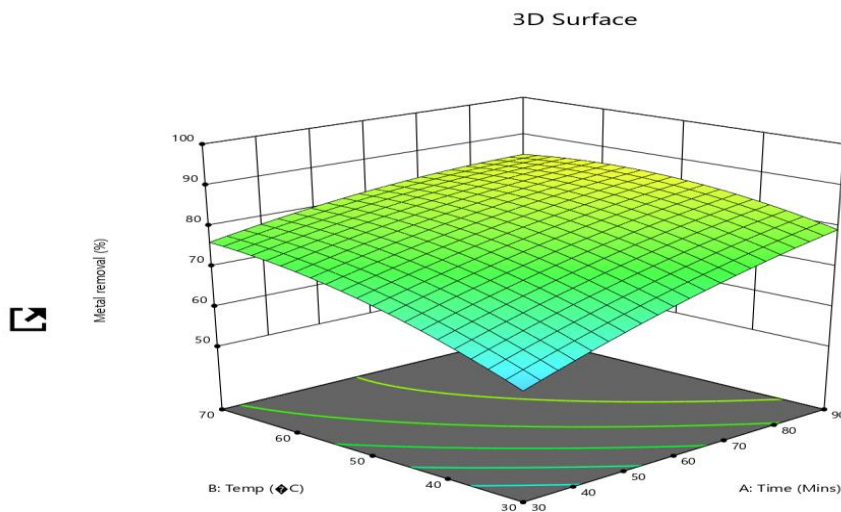


Figure 4.39: 3D plot of time and temperature interaction on % Pb removal

Factor Coding: Actual

Metal removal (%)

○ Design Points

50  99

X1 = A

X2 = B

Actual Factors

C = 0.3

D = Cd

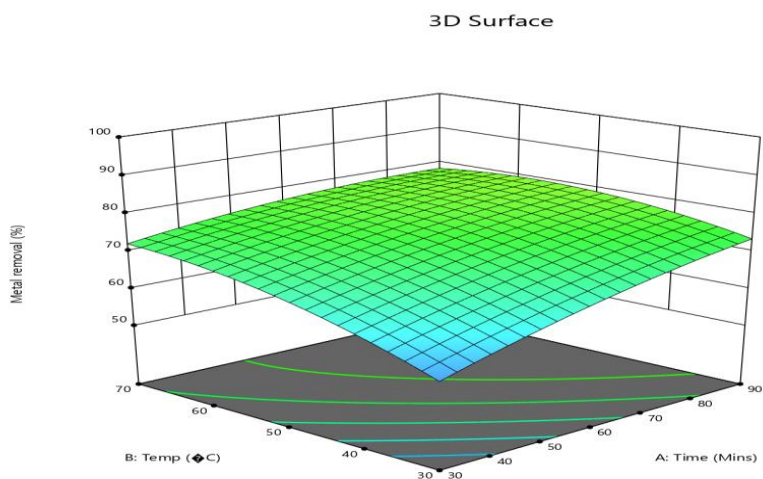


Figure 4.40 3D plot of time and temperature interaction on % Cd removal

Factor Coding: Actual

Metal removal (%)

○ Design Points

50  99

X1 = A

X2 = C

Actual Factors

B = 50

D = Pb

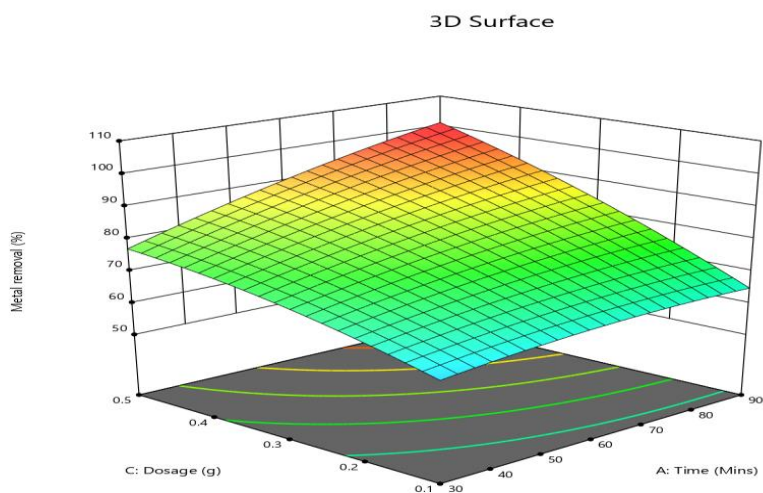


Figure 4.41: 3D plot of time and dosage interaction on % Pb removal

Factor Coding: Actual

Metal removal (%)

○ Design Points

50  99

X1 = A

X2 = C

Actual Factors

B = 50

D = Cd

Metal removal (%)

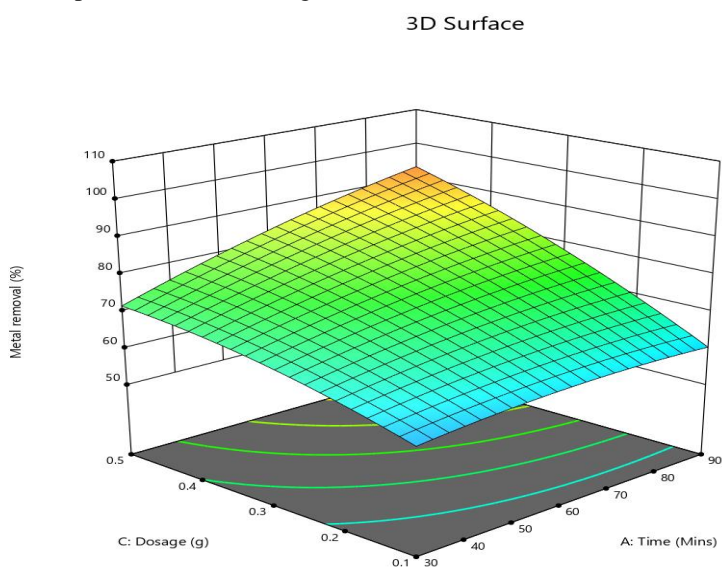


Figure 4.42: 3D plot of time and dosage interaction on % Cd removal

Factor Coding: Actual

Metal removal (%)

● Design Points

50  99

X1 = B

X2 = C

Actual Factors

A = 60

D = Pb

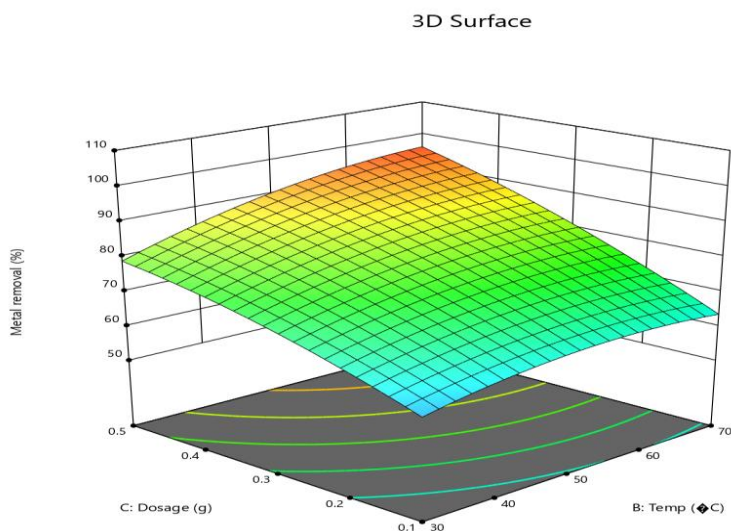


Figure 4.43: 3D plot of temperature and dosage interaction on % Pb removal

Factor Coding: Actual

Metal removal (%)

● Design Points

50  99

X1 = B

X2 = C

Actual Factors

A = 60

D = Cd

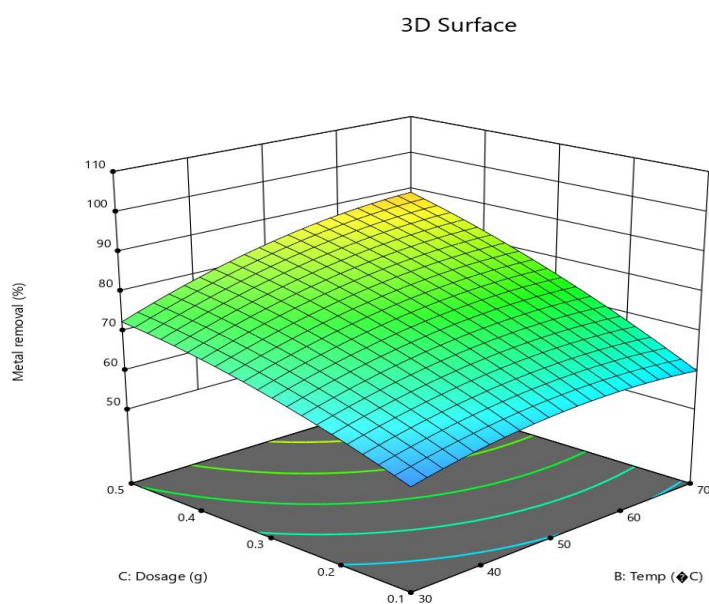


Figure 4.44: 3D plot of temperature and dosage interaction on % Cd removal

Model equations

Final Equation in Terms of Coded Factors

The model equation in coded form includes the constant term, the linear terms, interactive terms and quadratic terms:

$$\% \text{Metal removal} = 77.55 + 6.55A + 5.44B + 12.46C - 2.47D - 2.88AB + 4.87AC - 0.5658AD + 3.00BC - 0.1231BD - 0.8238CD - 1.74A^2 - 3.33B^2 - 2.36C^2 \quad (4.1)$$

Equation 4.1 contains both the significant and insignificant terms. When the non-significant terms are removed, the equation becomes:

$$\% \text{Metal removal} = 77.55 + 6.55A + 5.44B + 12.46C - 2.47D - 2.88AB + 4.87AC + 3.00BC - 1.74A^2 - 3.33B^2 - 2.36C^2 \quad (4.2)$$

The equation in terms of coded factors can be used to make predictions about the response for given levels of each factor. The coded equation is useful for identifying the relative impact of the factors by comparing the factor coefficients.

Final Equation in Terms of Actual Factors

$$\%Pb \text{ removal} = 10.36668 + 0.465027A + 1.1737B + 15.55926C - 0.004792AB + 0.8125AC + 0.75BC - 0.001934A^2 - 0.008329B^2 - 58.98809C^2 \quad (4.3)$$

$$\%Cd \text{ removal} = 10.76690 + 0.427306A + 1.16138B + 7.32174C - 0.004792AB + 0.8125AC + 0.75BC - 0.001934A^2 - 0.008329B^2 - 58.98809C^2 \quad (4.4)$$

The equation in terms of actual factors can be used to make predictions about the response for given levels of each factor. Here, the levels should be specified in the original units for each factor.

Optimum solution and validation of the two optimization experiments

Table 4.12: Optimum solution

Time (mins)	Temp (°C)	Dosage (g)	Metal type	Predicted Removal efficiency	Actual Removal efficiency	Error (%)
69.150	45.155	0.266	Pb	89.234	87.82	1.6
69.150	45.155	0.266	Cd	73.318	72.51	1.1

Design expert gave about 100 optimum solutions from which the predicted removal efficiency for each metal was selected. Experiments were carried out at these optimal reaction conditions to determine the actual adsorbent removal efficiency. The experiment is validated because there is an excellent agreement between the predicted and actual removal efficiency at the same condition.

V. CONCLUSIONS

The proximate analysis of the oil palm empty fruit bunch revealed that it has the requisite qualities for adsorbing contaminants from wastewater because of its rich fixed carbon content. Also, its exuberance and little or no other industrial application make it an excellent choice for treating pharmaceutical and other industrial wastewaters.

The AAS studies carried out revealed the presence of many heavy metals; however, all but lead and cadmium particles are within world health acceptable standard. The morphological analysis of oil palm bunch unveiled many vacant pores after chemical activation. These vacant spaces are effective sites for adsorption as the metal impurities could easily move to occupy them.

The most fitting isotherm models in this study for purging the wastewater are the Langmuir and Temkin while pseudo-2nd order kinetic model is the best kinetic model for describing the unwanted metals removal process.

Stirring time, temperature and dosage of the formulated adsorbent are the prevalent factors whose effects on the impurity removal were studied and optimized using RSM in order to achieve efficiency. These process factors influenced the wastewater treatment positively as increase in each within acceptable range is likely to increase the adsorbent adsorption capacity and removal efficiency. The optimization studies affirmed the significance of process conditions and suggested the most probable conditions for the removal of the metal impurities from the wastewater. At the established optimal process conditions, the predicted and actual removal efficiencies showed excellent relationship.

VI. RECOMMENDATIONS

Removal of heavy metal impurities from industrial effluents is extremely important prior to their release into the environment because most are carcinogenic.

While this review has successfully proven the efficacy of the selected biomass (oil palm empty fruit bunch) in decontamination of pharmaceutical wastewater, it is also recommended that further research should be conducted on:

- 1) The synthesizing of magnetic nano-based adsorbent particles from the activated oil palm empty fruit bunch through incorporation of magnetic materials into the activated oil palm bunch.
- 2) Methods of removing traces of the adsorbent from the treated wastewaters. This is one effective way of reducing the cost of synthesizing new adsorbents as the regenerated ones could still be used.
- 3) Nigeria government should make it a top priority that all our indigenous companies should make use of adsorbents produced from agro-based biomass for treating their industrial effluents.

REFERENCES

- [1]. Abasi, C.; Abia, A. and Igwe, J., (2011). Adsorption of iron (III), lead (II) and cadmium (II) ions by unmodified raphia palm (*Raphia hookeri*) fruit endocarp. *Environ. Res. J.*, 5(3): 104-113
- [2]. Abdullah, N. and Sulaiman, F. (2013). The thermal properties of the washed empty fruit bunches of oil palm. *Journal of Physical Science*, 24(2), 117 – 137.
- [3]. Abu Bakar, R., Darus, S.Z., Kulaseharan, S. and Jamaluddin, N. (2011). Effects of ten-year application of empty fruit bunches in an oil palm plantation on soil chemical properties. *Nutrient in Agro-ecosystems*, 89, 341 – 349.

- [4]. Acheampong MA, Meulepas RJ, Lens PN (2010). Removal of heavy metals and cyanide from gold mine wastewater, *Journal of Chemical Technology and Biotechnology*; 85(5): 590-613.
- [5]. Adebisi SA, Ipinromiti KO, Amoo IA (2007). Heavy Metals Contents of Effluents and Receiving Waters from Various Industrial Groups and their Environs. *J. Appl. Sci.*, 2(4): 345-348.
- [6]. Adeyanju, J.A., Ogunlakin, G.O., Adekunle, A.A., Alawode, G.E. and Majekolagbe, O.S. (2016). Optimization of oil extracted from coconut using response surface methodology. *J. Chem. Pharm. Res.*; 8 (1), 374–381
- [7]. Al-Anber, M., (2007). Removal of Iron (III) from model solution using Jordanian natural zeolite: magnetic study. *Asian J. Chem.*, 19(5): 3493–3501
- [8]. Al-Anber, M. and Al-Anber, Z.A., (2008). Utilization of natural zeolite as ion-exchange and sorbent material in the removal of iron. *Desalin.*, 225(1-3): 70-81
- [9]. Alslaibi TM, Abustan I, Ahmad MA, and Foul, A. A. (2013). Application of response surface methodology (RSM) for optimization of Cu²⁺, Cd²⁺, Ni²⁺, Pb²⁺, Fe²⁺, and Zn²⁺ removal from aqueous solution using microwaved olive stone activated carbon, *Journal of Chemical Technology and Biotechnology*; 88(12): 2141-2151.
- [10]. Aninwede O. Chukwuebuka; Egbuna O. Samuel; Christian O. Asadu; Ohimor E. Onoghwarite; Odenigbo Celestine and Chinonso A. Ezema (2021). Optimal analysis of the effects of process conditions on the yield of alkyl resin from castor and soybean seed oils using response surface methodology. *Chemical engineering journal advances*.
<https://doi.org/10.1016/j.cej.2021.100217>
- [11]. Asadu, O. Christian, Chinonso Anthony Ezema, Onu Chijioko Elijah, Nick O. Ogbodo, Onoh Ikechukwu Maxwell, Okachamma Franklin Ugwele, Aninwede S. Chukwuebuka, Thomas O. Onah, Evelyn Godwin-Nwakwasi, Innocent Sunday Ike and Ernest M. Ezech (2022). Equilibrium isotherm modelling and optimization of oil layer removal from surface water by organic acid grafted plantain pseudo stem fiber. *Case Studies in Chemical and Environmental Engineering* 5 100194
- [12]. Asadu, O. Christian, Samuel O. Egbuna, Thompson O. Chime, Chibuzor N. Eze, Kevin Dibia, Gordian O. Mbah, Anthony C. Ezema, Survey on solid wastes management by composting: optimization of key process parameters for biofertilizer synthesis from agro wastes using response surface methodology (RSM), *Artif. Intell. Agric.* 3 (2019) 52–56, <https://doi.org/10.1016/j.aiaa.2019.12.002>.
- [13]. Asadu, O. Christian, Samuel O. Egbuna, Thompson O. Chime, Chibuzor N. Eze, Dibia Kevin., Gordian O. Mbah and Anthony C. Ezema (2019), Survey on solid wastes management by composting: Optimization of key process parameters for biofertilizer synthesis from agro wastes using response surface methodology (RSM). *Artificial Intelligence in Agriculture* 3, 52–6
<https://doi.org/10.1016/j.aiaa.2019.12.002>
- [14]. Asadu, C.O., M.I. Onoh and C.A. Albert (2018a). Equilibrium isotherm studies on the adsorption of malachite green and lead ion from aqueous solution using locally activated ugwaka clay (black clay), *Archives of Current Research International* 12 (2) 1–11, <https://doi.org/10.9734/ACRI/2018/39302.ISSN:2454-7077>.
- [15]. Bagheri, H., A. Roostaie, and M. Baktash (2014). A chitosan-polypyrrole magnetic nanocomposite as μ -sorbent for isolation of naproxen,” *Analytica Chimica Acta*, vol. 816, pp. 1–7.
- [16]. Bakare AA, Lateef A, Amuda OS, Afolabi RO (2003). The aquatic toxicity and characterization of chemical and microbiological constituents of water samples from Oba River, Odo-oba, Nigeria.
- [17]. Benoff, S., Hauser, R., Marmar, J.L., Hurley I.R., Napolitano, B., and Centola G.M. (2009). Cadmium Concentrations in Blood and Seminal Plasma: Correlations with Sperm Number and Motility in Three Male Populations (Infertility Patients, Artificial Insemination Donors, and Unselected Volunteer. *15(7-8):248-262*.
- [18]. Cerro-Lopez M. and Méndez-Rojas M.A. (2017). Application of nanomaterials for treatment of wastewater containing pharmaceuticals. In *Ecopharmacovigilance*, Springer. Cham; 201-219.
- [19]. Che W, Luo Y, Deng F, et al. (2018). Facile solvothermal fabrication of cubic-like reduced graphene oxide/AgIn₅S₈ nanocomposites with anti-photocorrosion and high visible-light photocatalytic performance for highly-efficient treatment of nitrophenols and real pharmaceutical wastewater, *Applied Catalysis A: General*, 565;170-180.
- [20]. Che W, Luo Y, Deng F, et al. (2018). Facile solvothermal fabrication of cubic-like reduced graphene oxide/AgIn₅S₈ nanocomposites with anti-photocorrosion and high visible-light photocatalytic performance for highly-efficient treatment of nitrophenols and real pharmaceutical wastewater, *Applied Catalysis A: General*, 565;170-180.
- [21]. Chen Y, Wang C and Wang Z. (2005). Residues and source identification of persistent organic pollutants in farmland soils irrigated by effluents from biological treatment plants. *Environment International*, 31, 778–783.
- [22]. Chen, G., Chen, J., Srinivasakannan, C. and Peng, J. (2011). Application of response surface methodology for optimization of the synthesis of synthetic rutile from titania slag. *Appl. Surf. Sci.*; 258 (7), 3068–3073. <http://dx.doi.org/10.1016/j.apsusc.2011.11.039>
- [23]. Chimezie Anyakora, Kenneth Nwaeze, Olufunsho Awodele, Chinwe Nwadike, Mohsen Arbabi, and Herbert Coker (2011). Concentrations of heavy metals in some pharmaceutical effluents in Lagos, Nigeria. *Journal of Environmental Chemistry and Ecotoxicology* Vol. 3(2), pp. 25-31.
- [24]. Chinonso M. E. and Isaac O. I. (2012). Properties of oil palm empty fruit bunch fibre filled high density polyethylene. *International Journal of Engineering and Technology*. 2012; 6: 458-471.
- [25]. Coral Medina, J.D., Woiciechowski, A., Filho, A.Z., Nosedá, M.D., Kaur, B.S. and Soccol, C.R. (2015). Lignin preparation from oil palm empty fruit bunches by sequential acid/alkaline treatment – A Biorefinery approach. *Bioresource Technology*, 194, 172 – 178.
- [26]. Datta, S. (2011). Adsorption removal of chromium (VI) from aqueous solution over powdered activated carbon: optimization through response surface methodology. *J. Hazard. Mat.*; 173, 135–143. <http://dx.doi.org/10.1016/j.cej.2011.07.049>
- [27]. Denizli, A.; Say, R. and Arica, Y., (2000). Removal of heavy metal ions from aquatic solutions by membrane chromatography. *Sep. Purif. Tech.*, 21(1-2): 181-190
- [28]. Duffus HJ (2002). HEAVY METALS- A MEANINGLESS TERM? (IUPAC Technical Report); *Pure Appl.Chem.*, Vol.74, No.5, pp.793–807, 9(14)
- [29]. EFSA. (2009). Scientific Opinion of the Panel on Contaminants in the Food Chain on a request from the European Commission on cadmium in food. *EFSA J.* 980:1–144.
- [30]. EPA (2021). National primary drinking water regulations. <https://www.epa.gov/ground-water-and-drinking-water/national-primary-drinking-water-regulations#Organic>.
- [31]. Fawzy ME, Abdelfatta I, Abuarab ME, Mostafa E, Aboelghait KM, El-Awady MH, Sustainable approach for pharmaceutical wastewater treatment and reuse: Case study, *Journal of Environmental Science and Technology*, 2018; 11(4):209-19.

- [32]. Fazal, A, and Rafique, U. (2013). Severance of lead by acetylated and esterified spent camellia sinensis Powder, *Am. J. Environ. Eng.* 3 (6) 288–296, <https://doi.org/10.5923/j.ajee.2013.0306.04>.
- [33]. Gupta SK and Hung YT (2006). Treatment of pharmaceutical wastes. CRC Press/Taylor Francis Group: Boca Raton, Florida.
- [34]. Gupta, V.; Mittal, A.; Krishnan, L. and Gajbe, V. (2004). Adsorption kinetics and column operations for the removal and recovery of malachite green from wastewater using bottom ash. *Sep. Purif. Technol.*, 40(1): 87-96
- [35]. H.A. Omar, Adsorptive removal of phenol from aqueous solution using natural immobilized Chitin by Diathiazone, *New York Science Journal* 5 (8) (2012) 1–9.
- [36]. Ho YS (2004) Citation review of Lagergren kinetic rate equation on adsorption reactions. *Scientometrics* 59:171–177
- [37]. Ho, Y. S. and McKay, G. M. (1999). Pseudo second order model for sorption process. *Process Biochemistry*, Vol. 34, pp 451 – 465.
- [38]. Hounfodji, J., W. Kanhounon, G. Kpotin et al. (2021). Molecular insights on the adsorption of some pharmaceutical residues from wastewater on kaolinite surfaces,” *Chemical Engineering Journal*, vol. 407, p. 127176.
- [39]. Huerta-Fontela, M., M. Galceran, and F. Ventura (2011). Occurrence and removal of pharmaceuticals and hormones through drinking water treatment,” *Water Research*, vol. 45, no. 3, pp. 1432–1442.
- [40]. Hussein S. Mohamed, N. K. Soliman, Doaa A. Abdelrheem, Arwa A. Ramadan, Ahmed H. Elghandour and Sayed A. Ahmed (2019). Adsorption of Cd²⁺ and Cr³⁺ ions from aqueous solutions by using residue of *Padina gymnospora* waste as promising low-cost adsorbent. *Heliyon* 5 e01287. doi: 10.1016/j.heliyon.2019. e01287
- [41]. Idris, S.S., Rahman, N.A., Ismail, K., Alias, A.B., Rashid, Z.A. and Aris, M.J. (2010). Investigation on thermochemical behaviour of low rank Malaysian coal, oil palm biomass and their blends during pyrolysis via thermogravimetric analysis (TGA). *Bioresource Technology*, 101, 4584 – 4592.
- [42]. Janice May Lynn Thoe, Noumie Surugau and Harry Lye Hin Chong (2019). Application of Oil Palm Empty Fruit Bunch as Adsorbent: A Review. *Transactions on Science and Technology* Vol. 6, No. 1, 9 –26 493 - 501.
- [43]. Joseph T. Nwabanne, Chijioke E. Onu, Okwudili C. Nwankwoukwu, Equilibrium, kinetics and thermodynamics of the bleaching of palm oil using activated Nando clay, *Journal of Engineering Research and Reports* 1 (3) (2018b) 1–13, <https://doi.org/10.9734/JERR/2018/42699>
- [44]. Kong D. (2009). Master Thesis, Department of land and water resources engineering. Royal Institute of Technology (KTH), SE-100 44 STOCKHOLM, Sweden.
- [45]. Lee CM, Palaniandy P, Dahlan I. (2017). Pharmaceutical residues in aquatic environment and water remediation by TiO₂ heterogeneous photocatalysis: a review, *Environmental Earth Sciences*, 76(17):611.
- [46]. Liu, H.; Feng, S.; Zhang, N.; Du, X. and Liu, Y., (2013). Removal of Cu(II) ions from aqueous solution by activated carbon impregnated with humic acid . *Front . Environ. Sci. Eng.*, 8(3): 329-336
- [47]. Liu, Y., L. Rong, L. Ming, Y. Fucheng, and C. He (2019). Removal of pharmaceuticals by novel magnetic genipin-crosslinked chitosan/graphene oxide-SO₃H composite. *Carbohydrate Polymers*, vol. 220, pp. 141–148.
- [48]. Loredó-Cancino M, Soto-Regalado E, García-Reyes RB, et al. (2016). Adsorption and desorption of phenol onto barley husk-activated carbon in an airlift reactor. *Desalination and Water Treatment*, 57(2) :845-860.
- [49]. Mahjoub, R., Yatim, J.B.M. and Sam, A.R.M. (2013). A review of structural performance of oil palm empty fruit bunch fibre in polymer composites. *Advances in Materials Science and Engineering*, 2013, 1 – 9.
- [50]. Manohar, D.M., Noeline, B.F., Anirudhan, T.S. (2006). Adsorption performance of Al-pil-lared bentonite clay for the removal of cobalt(II) from aqueous phase. *Appl. Clay Sci.* 31, 194-206.
- [51]. Memon, S.Q.; Memon, N.; Shah, S.; Khuhawar, M.; Bhangar, M. (2007). Sawdust—A green and economical sorbent for the removal of cadmium (II) ions. *J. Hazard. Mater.* 139, 116–121.
- [52]. Mnasri-Ghnnimi and Frini-Srasra (2019). Removal of heavy metals from aqueous solutions by adsorption using single and mixed pillared clays. *Applied clay science* 179 105151.
- [53]. Mohamad Nor, N.; Lau, L.C.; Lee, K.T.; Mohamed, A.R. Synthesis of activated carbon from lignocellulosic biomass and its applications in air pollution control—A review. *J. Environ. Chem. Eng.* 2013, 1, 658–666.
- [54]. Mohammadpour, G.H.A.; Karbassi, A.R.; Baghvand, R., (2016b). A pollution index for agricultural soils. *Arch. Agro. Soil Sci.*, 62(10): 1411-1424
- [55]. Mohammed, M.A.A., Salmiaton, A., Wan Azlina, W.A.K.G. and Mohamad Amran, M.S. (2012). Gasification of oil palm empty fruit bunches: A characterisation and kinetic study. *Bioresource Technology*, 110, 628 – 636.
- [56]. Momodu M and Anyakora C (2010). Heavy Metal Contamination of Groundwater: The Surulere Case Study. *Res. J.Environ. Earth Sci.*,2(1):39-43.
- Montgomery, D.C. (2004). Design and analysis of experiments. John Wiley & Sons, Inc., New York.
- [57]. Monu A, Bala K, Shweta R, Anchal R, Barinder K and Neeraj M (2008). Heavy metal accumulation in vegetables irrigated with water from different sources. *Guru Jambheshwar University of Science and Technology, Hisar (Haryana)* 125 001, India.
- [58]. Moreno-Castilla, C. and Rivera- Utrilla, J.(2001). Carbon materials as adsorbents for the removal of pollutants from the aqueous phase. *MRS Bull. MRS Bulletin*, 26(11): 890-894
- [59]. Moriguchi, T.; Yano, K.; Tahara, M. and Yaguchi, K., (2005). Metal-mod ifi ed silica adsorbents for removal of humic substances in water. *J. Colluid Interf. Sci.*, 283(2): 300-310
- [60]. Saad, R.; Hamoudi, S. and Belkacemi, K., (2007). Adsorption of phosphate and nitrate anions on ammonium-functionnalized mesoporous silicas. *J. Porous. Mater.*,15(3): 315-323
- [61]. Mortazavian S, An H, Chun D, Moon J. (2018). Activated carbon impregnated by zero-valent iron nanoparticles (AC/nZVI) optimized for simultaneous adsorption and reduction of aqueous hexavalent chromium: Material characterizations and kinetic studies, *Chemical Engineering Journal*; 353: 781-795
- [62]. Motsi, T.; Rowson, N.; Simmons, M., (2009). Adsorption of heavy metals from acid mine drainage by natural zeolite. *Int. J. of Miner. Proc.*, 92(1-2): 42-48
- [63]. Muchuweti M, Birkett JW, Chinyanga E, Zvauya R, Scrimshaw MD and Lester JN (2006). Heavy metal content of vegetables irrigated with mixture of wastewater and sewage sludge in Zimbabwe: implications for human health. *Agriculture, Ecosystem and Environment*, 112, 41–48.
- [64]. Myers, R.H. and Montgomery, D.C. (2002). Response surface methodology process and product optimization using design of experiments, John Wiley and Sons, New York, pp. 798.
- [65]. Nabais, R. (2006). Odours prevention in the food industry. *Odors Food Ind.*, 75-104
- [66]. Naseem, R. and Tahir, S. S. (2001). Removal of Pb(II) from aqueous solution by using bentonite as an adsorbent. *Water. Res.* 35, 3982–3986.

- [67]. Nick O. Ogbodo, Christian O. Asadu, Chinonso Anthony Ezema, Maxwell I. Onoh, Onu Chijioko Elijah, Sunday InnocentIke, OhimorEvuensiriOnoghwarite, Preparation and Characterization of activated carbon from agricultural waste (Musa-paradisiacapeels) for the remediation of crude oil contaminated water, *J. Hazard. Mater. Adv.* (2021), <https://doi.org/10.1016/j.hazadv.2021.100010>.
- [68]. Nordberg, G.F.; Fowler, B.A.; Nordberg, M.; Friberg, L., (2007). Removal of synthetic dyes from wastewaters: A review. *Environ. Int.*, 30(7): 953-971
- [69]. Nordin NIAA, Ariffin H, Andou Y, Hassan MA, Shirai Y, Nishida H, Yunus WMZW, Karuppuchmy S, Ibrahim NA. (2013). Modification of oil palm mesocarp fiber characteristics using superheated steam treatment. MDPI AG.
- [70]. Okpe Emmanuel Chinonye, Asadu Christian Oluchukwu and Onu Chijioko Elijah (2018): Statistical analysis for orange G adsorption using kola nut shell activated carbon, *Journal of the Chinese Advanced Materials Society*. <https://doi.org/10.1080/22243682.2018.1534607>
- [71]. Oluyemi, E.A., Oyekunle, J.A.O. and Olasoji, S.O. (2009). A Comparative Study of Heavy Metals Removal from Synthetic Wastewaters Using Different Adsorbents, *Adsorption Science and Technology* 27(5).
- [72]. Parshetti, G.K., Hoekman, S.K. and Balasubramanian, R. (2013). Chemical, structural and combustion characteristics of carbonaceous products obtained by hydrothermal carbonization of palm empty fruit bunches. *Bioresource Technology*, 135, 683 – 689.
- [73]. Perez-Vega, S.; Ortega-Rivas, E.; Salmeron-Ochoa, I.; Sharratt, P. N. (2012). A system view of solvent selection in the pharmaceutical industry: Towards a sustainable choice. *Environ., Dev. Sustainability*, 15 (1), 1–21.
- [74]. Qin W, Song Y, Dai Y, Qiu G, Ren M, Zeng P.(2015). Treatment of berberine hydrochloride pharmaceutical wastewater by O3/UV/H2O2 advanced oxidation process, *Environmental earth sciences*, 2015; 73(9):4939-4946.
- [75]. Quak P. and Knoef H. (1999). "Energy from Biomass-A Review of Combustion and Gasification Technologies." WB Technical Paper No 422-Energy Series
- [76]. Rajeshkannan, R., M. Rajasimman and N. Rajamohan (2011). Decolourisation of malachite green using tamarind seed: optimisation, isotherm and kinetic studies, *Chem. Ind. Chem. Eng. Q.* 17 (1) 67–79.
- [77]. Rabiul Aual Muhammed, Md MunjurHasan, A novel fine-tuning mesoporous adsorbent for simultaneous lead(II) detection and removal from wastewater-, *Sensor. Actuator. B Chem.* 202 (2014) 395–403.
- [78]. Rana RS, Singh P, Kandari V, Singh R, Dobhal R. and Gupta S. (2017). A review on characterization and bioremediation of pharmaceutical industries' wastewater: an Indian perspective, *Applied water science*, 7(1); 1-12.
- [79]. Rangsayatorn, N.; Pokethitiyook, P.; Upatham, E. and Lanza, G. (2004). Cadmium bio-sorption by cells of spirulina platensis TISTR 8217 immobilized in alginate and silica gel. *Environ. Int.*, 30(1): 57-63
- [80]. Arivoli, S., M. Hema and P.D. Martin (2009). Adsorption of malachite green onto carbon prepared from Borassus bark, *Arabian J. Sci. Eng.* 34 (2A) 31–43
- [81]. Saeed, A., Iqbal, M. and Akhtar, M. W. (2005). Removal and recovery of lead (II) from single and multimetal (Cd, Cu, Ni, Zn) solutions by crop milling waste (black gram husk)", *Journal of Hazardous Materials*, Vol., Number, pp.
- [82]. Salleh MAM, Mahmoud DK, Karim WAWA, Idris A (2011) Cationic and anionic dye adsorption by agricultural solid wastes: a comprehensive review. *Desali* 280:1–13
- [83]. Sankha, B. (2021). Central Composite Design for Response Surface Methodology and Its Application in Pharmacy [Online First], *IntechOpen*, DOI: 10.5772/intechopen.95835
- [84]. Sarici-Özdemir, C. and Önal, Y. (2010). Study to investigate the importance of mass transfer of naproxen sodium onto activated carbon," *Chemical Engineering Process: Process Intensification*, vol. 49, no. 10, pp. 1058–1065.
- [85]. Sarin, P.; Snoeyink, V.; Bebee, J.; Jim, K.; Beckett, M.; Kriven, W. and Clement, J. (2004). Iron release from corroded iron pipes in drinking water distribution systems: Effect of dissolved oxygen. *Water Res.*, 38 (5): 1259 -1269
- [86]. Shao, L., R. Zongming, Z. Gaosheng, and C. Linlin (2012). Facile synthesis, characterization of a MnFe₂O₄/activated carbon magnetic composite and its effectiveness in tetracycline removal. *Materials Chemistry and Physics*, vol. 135, no. 1, pp. 16–24.
- [87]. Shariff, A., Aziz, N.S.M. and Abdullah, N. (2014). Slow pyrolysis of oil palm empty fruit bunches for biochar production and characterisation. *Journal of Physical Science*, 25(2), 7 – 112.
- [88]. Shirafkan A, Nowee SM, Ramezani N. and Etemadi MM (2016). Hybrid coagulation/ozonation treatment of pharmaceutical wastewater using ferric chloride, polyaluminum chloride and ozone, *International journal of environmental science and technology*, 13(6): 1443-1452.
- [89]. Singh KP, Mohan D, Sinha S and Dalwani R. (2004). Impact assessment of treated/ untreated wastewater toxicants discharged by sewage treatment plants on health, agricultural, and environmental quality in the wastewater disposal area. *Chemosphere*, 55, 227–255.
- [90]. Sitre S., Dhadse S. and Satyanarayan S. (2009). Toxicity of herbal pharmaceutical wastewater to a freshwater crustacean *Ceriodaphnia dubia*, *Bulletin of environmental contamination and toxicology*; 82(3): 275-279.
- [91]. Soliman, N. and A. Moustafa (2020). Industrial solid waste for heavy metals adsorption features and challenges; a review," *Journal of Materials Research and Technology*, vol. 9, no. 5, pp. 10235–10253.
- [92]. Sui, Q., X. Cao, S. Lu, W. Zhao, Z. Qiu, and G. Yu (2015). Occurrence, sources and fate of pharmaceuticals and personal care products in the groundwater: a review," *Emerging Contaminants*, vol. 1, no. 1, pp. 14–24.
- [93]. Taran, M. and Aghaie, E. (2015). Designing and optimization of separation process of iron impurities from kaolin by oxalic acid in bench-scale stirred-tank reactor. *Applied Clay Science*, 107. <http://dx.doi.org/10.1016%2Fj.clay.2015.01.010>
- [94]. U.V. Ladhe, S.K. Wankhede, V.T. Patil, P.R. Patil, Adsorption of eriochrome blackT from aqueous solutions on activated carbon prepared from mosambi peel, *J. Appl. Sci. Environ. Sanit.* 6 (2) (2011) 149–154.
- [95]. Ugwele, F.O.; Aninwede, C.S.; Chime, T.O.; Asadu, C.O. and Ike, S. I. (2020). Application of Response Surface Methodology in Optimizing the Process Conditions for the Regeneration of Used Mobil Oil using different kinds of Acids. *Heliyon journal*, Elsevier Ltd. <https://doi.org/10.1016/j.heliyon.2020.e05062>
- [96]. Uzoh, C. F.; Onukwuli, O.D.; Odera, R.S. and Ofochebe, S. (2013). Optimization of polyesterification process for production of palm oil modified alkyd resin using response surface methodology. *Journal of Environmental Chemical Engineering* 1 (2013) 777–785. <http://dx.doi.org/10.1016/j.jece.2013.07.021>
- [97]. Wahi, R., Ngaini, Z., & Jok, V. (2009). Removal of mercury, lead and copper from aqueous solution by activated carbon of palm oil empty fruit bunch. *World Applied Sciences Journal*, 5, 84– 91.

- [98]. Wan g, S. and Peng, Y. (201 0). Natural zeolites as effective adsorbents in water and wastewater treatment. *Chem. Eng. J.*, 156(1): 11-24
- [99]. Wang, H.; Kang, J.; Liu, H. and Qu, J., (2009). Preparation of organically functionalized silica gel as adsorbent for copper ion adsorption. *J. Environ. Sci.*, 21(1 1): 147 3-1 479
- [100]. Wei, X., Y. Wang, J. and Chen et al. (2020). Adsorption of pharmaceuticals and personal care products by deep eutectic solvents-regulated magnetic metal-organic framework adsorbents: performance and mechanism,” *Chemical Engineering Journal*, vol. 392, p. 124808.
- [101]. WHO (2006). *Guidelines for drinking-water quality*, World Health Organization, 4th edition.
- [102]. Yang, C. L. and McGarrahian, J. (2005) . Electrochemical coagulation for textile effluent decolorization. *J. Hazard. Mater.*, 117: 171-178
- [103]. Yang, H., Yan, R., Chin, T., Liang, D.T., Chen, H. and Zheng, C. (2004). Thermogravimetric analysis–Fourier transform infrared analysis of palm oil waste pyrolysis. *Energy & Fuels*, 18, 1814 – 1821.
- [104]. Yiping G and Yu B (2010). *Advanced Treatment and Recycling Technology of Wastewater Treatment Plant* (China Architecture Press) pp 198-206.
- [105]. Yu Y (2013). *Experimental on Pharmaceutical Tail Water before Biochemical Pretreatment* (Changchun: Jilin University) pp 12-9
- [106]. Yu, B., B. Yitong, M. Zhu et al. (2017). Adsorption behaviors of tetracycline on magnetic graphene oxide sponge. *Materials Chemistry and Physics*, vol. 198, pp. 283–290.
- [107]. Zakir, H., S. Sharmin, A. Akter, and M. Rahman (2020) Assessment of health risk of heavy metals and water quality indices for irrigation and drinking suitability of waters: a case study of Jamalpur Sadar area, Bangladesh,” *Environmental Advances*, vol. 2, p. 100005.
- [108]. Zhang, X.; Gao, B.; Creamer, A.E.; Cao, C.; Li, Y. Adsorption of VOCs onto engineered carbon materials: A review. *J. Hazard. Mater.* 2017, 338, 102–123
- [109]. Zhu, F., Y. Zheng, B. Zhang, and Y. Dai (2021). A critical review on the electrospun nanofibrous membranes for the adsorption of heavy metals in water treatment,” *Journal of Hazardous Materials*, vol. 401, p. 123608.